Microwave catalytic depolymerisation of PET plastic via glycolysis

Journal:	*CCS Chemistry*
Manuscript ID	CCSC-2023-03089
Manuscript Type:	Research Article
Date Submitted by the Author:	02-Jun-2023
Complete List of Authors:	Tang, Junwang; University College London; Tsinghua University Yuan, Zhe; University College London Yang, Jianlong ; Northwest University George, Manos; University College London
Keywords:	plastic waste, Microwave, glycolysis, microwave absorbing catalyst, PET depolymerisation
Subject Interest:	Catalytic Chemistry < Catalysis and Surface/ Interface Chemistry
Speciality:	

Microwave catalytic depolymerisation of PET plastic via glycolysis

Abstract

Plastic waste management has emerged as a critical environmental issue due to the exponential increase in plastic consumption worldwide. Polyethylene terephthalate (PET) is extensively used in the production of water bottles, which constitutes a significant fraction of the plastic waste. PET recycling is a challenging task due to the lack of efficient and cost-effective depolymerisation methods. In this study, we developed a microwave (MW) catalytic depolymerisation method for PET recycling using modified zinc oxide loaded with manganese oxide as a co-catalyst. The modified Mn3O4/ZnO catalyst presents high efficiency in depolymerising PET into its monomers with only 0.4 wt% ratio of the catalyst to PET, resulting in 100% conversion of PET and 88% selectivity towards BHET monomers operated at 175°C for 5 minutes. It is believed that Mn_3O_4 provides additional Lewis acid sites, promoting the dissociation of glycol from PET, and the MW irradiation plays a crucial role in rapidly heating the ethylene glycol and the catalyst, thereby accelerating the PET depolymerisation process. In addition, the heterogeneous nature of the catalyst facilitates its easy separation from the reaction mixture for reuse, simplifying the catalyst recovery process and enabling the process cost-effective and sustainable for PET recycling. Thus this study provides an innovative and sustainable solution for PET recycling, contributing towards the circular economy and mitigating the environmental impact of the plastic waste.

1. Introduction

The plastic production is undoubtedly one of the most significant innovations in human history. Ever since the invention of the first man-made plastic, Parkesine (nitrocellulose) by Alexander Parke in 1856[1], numerous plastics with novel properties have been invented and widely utilized. However, the technical innovations that led to the development and proliferation of plastics did not sufficiently consider their long-term impact on the environment.

Polyethylene terephthalate (PET) is an engineering thermoplastic with excellent chemical and physical properties, making it one of the most prevalent types of plastics in our daily lives. PET production reaches almost 70 million tons annually worldwide[2] and it is mainly used for packaging applications, such as water bottles and carbonated soft drink containers, an additive in polyester fabrics in the textile industry, and films in tape applications. While plastics have brought numerous benefits to society, the environmental impact of their widespread usage cannot be ignored. The technology to lower ecological footprints of the plastic use should be pursued.

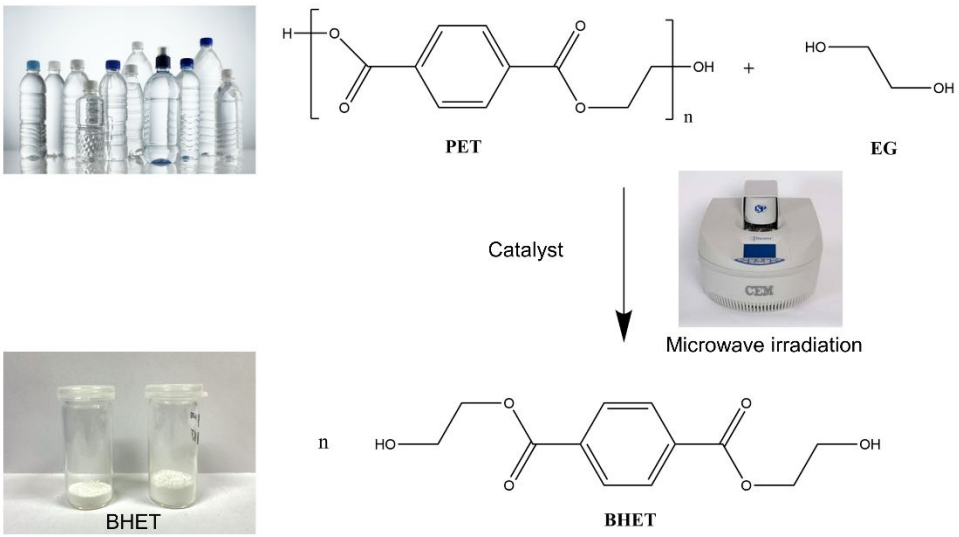

Figure 1. The general procedure of PET glycolysis

PET waste is, in particular, difficult to naturally degrade due to its high resistance to atmospheric and biological agents. As PET drinking bottles are typically single-use, the lack of effective recycling methods results in the widespread pollution of the environment. This has significant consequences for the living world, particularly marine life. The annual cost of the waste plastic in the marine environment is estimated to be over $13 billion[3], with the plastic pollution crisis being linked to that posed by CO_2 to climate change by the Environmental Investigation Agency (EIA)[4]. Therefore, it is crucial to decrease both plastic production and its waste, and to address the disposal of PET waste has become an urgent environmental issue that requires immediate action. Primary recycling, secondary or mechanical recycling, and tertiary or chemical

recycling are three accessible recycling processes for PET waste[5,6]. Primary recycling pertains to reprocessing low-grade industrial waste that fails to meet the desired quality standard, whereas secondary recycling involves segregating PET materials from contaminants and reusing them by melt extrusion into granules[7]. Chemical recycling, which is a widely accepted and sustainable approach, converts PET into its monomer or secondary value-added products. With different solvents, three main methods could be distributed hydrolysis[8], methanolysis[9], and glycolysis[10]. The main products from each method are terephthalic acid (TPA), dimethyl terephthalate (DMT), and bis-hydroxyethyl terephthalate (BHET), respectively. Methanolysis and hydrolysis are two common chemical processes used for the breakdown of various compounds. Despite their usefulness, these processes are often associated with significant drawbacks such as high reaction temperatures, high pressures[11,12], and the use of homogeneous catalysts[5], which can be harsh and environmentally damaging.

The glycolysis of PET is a method using ethylene glycol (EG) as a solvent for PET depolymerisation[13]. The general procedure of PET glycolysis is shown in Figure 1. The resulting product of PET glycolysis is BHET, which can be purified and used in the production of new PET products or other chemicals. The glycolysis of PET usually takes a long-drawn process without the catalyst[13]. The rate of degradation is low and oligomer from the degradation of PET has a higher selectivity than BHET. Hence, finding efficient procedures and the catalysts to enhance glycolysis yield has become the goal of research in the last decades.

Various catalysts, both homogeneous and heterogeneous, have been investigated for PET glycolysis. Homogeneous catalysts, including metal acetates (with an active order: Zn^{2+}> Mn^{3+} > Co^{2+} >Pb^{2+}) [14,15], metal carbonates (with an active order: Na_2CO_3> $NaHCO_3$) [16], metal sulfates (with an active order: Zn^{2+}> Na^{+}> K^{+})[17], and metal chlorides acetates (with an active order: Zn^{2+}> Nd^{3+} > Li^{2+}> Fe^{2+} > Mg^{2+})[13], have shown high catalytic performance, achieving 100% PET conversion and over 70% BHET yield. Although these homogeneous catalysts have been reported to exhibit high catalytic performance, they still have disadvantages of separation, recyclability, low purity of products[18]. The heterogeneous catalysts offer several advantages over homogeneous counterparts, including increased sustainability, ease of recovery and recycling, and improved tolerance to changes in reaction conditions[13]. Several pioneering and insightful works have been dedicated to this area. For example, the graphene oxide (GO) nanoparticles supported metal oxides was synthesised as the heterogeneous catalysts for PET glycolysis[19]. The GO was used as a large surface supporter to modify the stability of Mn_3O_4. The highest yield (96.4%) of BHET was obtained by using 41 wt% GO-Mn_3O_4 (41 wt% Mn_3O_4 of entire GO-Mn_3O_4) operated at 300°C and 1.1 MPa for 80 minutes. Mixed metal oxide spinels ($ZnMn_2O_4$, $CoMn_2O_4$, $ZnCo_2O_4$) were also investigated as the catalysts in the glycolysis of PET[20]. The highest yield (92.2%) was obtained using $ZnMn_2O_4$ under optimised reaction condition at 260°C for 60 minutes with 1 wt% the catalyst and EG/ PET ratio of 17.2. The study indicated that mixed metal oxides would perform a better catalytic activity than traditional metal oxides. (Mg–Zn)–Al layered double hydroxide was also synthesized as a regenerable

heterogeneous catalyst for glycolysis of PET[21]. The study indicated that (Mg–Zn)–Al layered double hydroxide catalyst achieved 100% PET conversion and 75% BHET yield at 190°C after 3 hour run. The catalytic activity did not decrease significantly after 5 cycles. Despite the outstanding advantages of heterogeneous catalysts, the relatively high temperature, high pressure, in particular long reaction time are significant challenges to the large scale commercial application of PET glycolysis.

Alternatively， microwave irradiation has been considered as an ideal heating source to shorten the reaction time, combined with MW absorber catalysts. Numerous studies have compared microwave heating with conventional heating in glycolysis of PET[22–24]. For instance, an 800W domestic microwave oven was employed for conducting PET glycolysis[22]. In order to assess the variance in PET glycolysis between conventional electric heating and microwave heating, zinc acetate was selected as the catalyst owing to its notable catalytic efficacy. The reaction duration was significantly reduced from 8 hours to a mere 35 minutes, while achieving a comparable BHET yield of 66%. The study conclusively indicated that microwave heating effectively reduces the reaction time. However the microwave power was too high. To comprehensively investigate the role of microwave heating in the PET glycolysis reaction and make an economic method for PET recycling, it is imperative to gain a deep understanding of the MW's function in this process.

In this study, a novel and efficient catalytic route for glycolysis of PET into BHET was developed. The temperature of MW heating was closely monitored and systematically compared to conventional heating methods. The proposed synergistic strategy involves the combined use of a cocatalyst, a microwave catalyst, and selective MW heating. The use of a MW-absorbing catalyst was found to be crucial in the catalytic reaction, resulting in highly localized and intense heating that generated specific hot spots on the catalyst. Among the various MW catalysts tested, the best catalytic performance was achieved over 10wt% Mn/ZnO. The combination of the catalyst with an appropriate solvent resulted in a highly active catalytic system for the depolymerisation of PET with 100% conversion and 87.9% yield to the monomer in 5 min reaction time, which is found to be more efficient, much faster, and more selective compared to conventional heating and other catalysts reported, thus providing a promising approach for large-scale BHET production from PET depolymerisation. Furthermore, the reaction mechanism was also discussed.

2. Experimental methods

Materials and Microwave system

Commercial water bottles (Marks & Spencer, UK) were collected as raw materials. The water bottles were first cut into small flakes, approximately 3mm by 3mm in size. The PET flakes were washed by ethanol and deionized water in the ultrasonic machine 3 times, then dried in oven at 60°C for 24 hours. Ethylene glycol (≥99%, reagent plus) was used as obtained from Sigma-Aldrich. Commercial metal salts and metal oxides were purchased from Sigma-Aldrich.

The microwave irradiation system (CEM Discover SP) was equipped with temperature and pressure sensors. The maximum operating power is 300W and the safety pressure is set at 250 psi (17.24 bar). The operation power was set to 200W.

Preparation of Mn/ZnO

The cocatalysts were added on commercial ZnO (Sigma-Aldrich) by an incipient impregnation method[25]. In detail, analytical grade $Mn(NO_3)_2 \cdot 4H_2O$ (Sigma-Aldrich) was dissolved in deionized water, and the metal precursor solution was added dropwise to ZnO. The mixtures were dried in oven at 60°C for 24 hours. After drying, the precursors were calcined at 400°C in the air atmosphere for 2 hours. Other transition metal oxides were also prepared by the same method. The prepared catalyst was denoted 10 wt% Mn/ZnO, 10 wt% Fe/ZnO, 10 wt% Cu/ZnO, 10 wt% Ni/ZnO.

Procedure of catalytic PET glycolysis

The reaction was operated in a 10mL sealed vessel. 0.5g of PET, 0.002g catalyst, and 5g EG were added into a 10mL vessel. Then it was put into ultrasonic machine for 10 minutes to disperse the catalyst particles in EG solvent. A magnetic rotor was added into the vial and stirred all the time throughout the microwave reaction. The maximum power of the microwave was set at 200W unless otherwise stated. The holding temperature was 175°C and holding time was 5 minutes. The power would change dynamically to keep the reaction temperature.

After the reaction, 50mL of distilled water were added while vigorously stirring at 70°C for 30minutes to extract BHET from the mixture. The unreacted PET flakes were removed, dried, and weighted. Another insoluble fraction in water was a mixture of oligomers formed during the reaction and catalysts, which was filtered, dried, and weighted. The filtrate was firstly stored at -10℃ for 12 hours to improve the recrystallisation of BHET. To separate BHET from solution, the low temperature filtrate was defrosted and filtered rapidly to avoid BHET re-dissolving. Collected products were dried in oven at 60°C for 12 hours and then weighed as target product BHET.

Measurement of catalytic activity

PET conversion and the yield to products are two major factors to define the catalytic performance of a catalyst herein.

The conversion of PET was calculated by the following formula:

$$\boldsymbol{Conversion\ of\ PET} = \frac{m_{PET,\,0} - m_r}{m_{PET,0}} \times 100\%$$

where $m_{PET,0}$ and m_r refer to the initial mass of PET, mass of the solid residue, respectively.
The yield of BHET was calculated by using the following formula:

$$\boldsymbol{Yield\ of\ BHET} = \frac{\frac{m_{BHET}}{M_{BHET}}}{\frac{m_{PET,\,0}}{M_{PET,\,unit}}} \times 100\%$$

Where m_{BHET}, M_{BHET}, and $M_{PET,0}$ refer to mass of collected BHET, molecular mass of BHET (254/mol), and molecular mass of repeating PET units (192g/mol), respectively.

Catalyst recycling

To evaluate the recycling of our catalysts to make the process more cost-effective and sustainable, five reaction cycles were carried out with the used catalyst under the optimised conditions. As some catalyst might inevitably be lost during the filtration process, in order to maintain the optimal catalyst: PET ratio, we proportionally reduced the mass of PET and the amount of EG according to the mass of the recycled catalyst. In case of incomplete conversion, we transferred the solid residue remained after the filtration to the next cycle to save raw materials.

Characterisation

Nuclear magnetic resonance (NMR) spectra of the main products were recorded on a Bruker Advance 300WB spectrometer (Bruker) with 4 mm magic-angle spinning probe, respectively in DMSO-d6 solution. Fourier transform infrared spectroscopy (FTIR) spectra of the products were performed via a Vertex 70 ATR-FTIR Spectrometer (Bruker). Thermogravimetric analysis (TGA) of products were carried out on a Perkin Elmer TGA 7 Thermogravimetric Analyzer (Perkin Elmer) from 25 °C to 600 °C at a rate of 10 °C min^{-1} under a nitrogen atmosphere.

X-ray photoelectron spectrometer (XPS) spectra of the catalysts before and after the reaction were collected with the instrument of Thermo Scientific XPS K-alpha (Thermo Fisher Scientific). X-ray diffraction (XRD) of main products and catalysts were conducted in a Stoe Stadi-P Cu diffractometer with Mythen1K & CryojetHT (STEO). The Joel 2100 transmission electron microscopy (TEM) with an Oxford instruments energy-dispersive X-ray (EDX) detector (Joel) were used to visualize the structure in matter.

3. Results and discussion

Different catalysts were prepared and screened to obtain the effective one. The catalyst ZnO loaded with various transition metal oxides were first tested for the glycolysis of PET and the results are shown in Figure 2 (a). ZnO shows 24.2% conversion of PET and 19.2% selectivity to BHET. When adding Fe, Cu, Ni, and Mn as a cocatalyst to ZnO, the conversion are shown in the following order: Mn/ZnO (100%) > Ni/ZnO (32.2%) > Cu/ZnO (28.1%) > Fe/ZnO (25.2%). Among the catalysts tested, manganese oxides loaded on ZnO shows the significant improvement of the catalytic activity, with a PET conversion rate of 100% and a BHET yield of 87.9% achieved only after 5 minute reaction at 175°C.

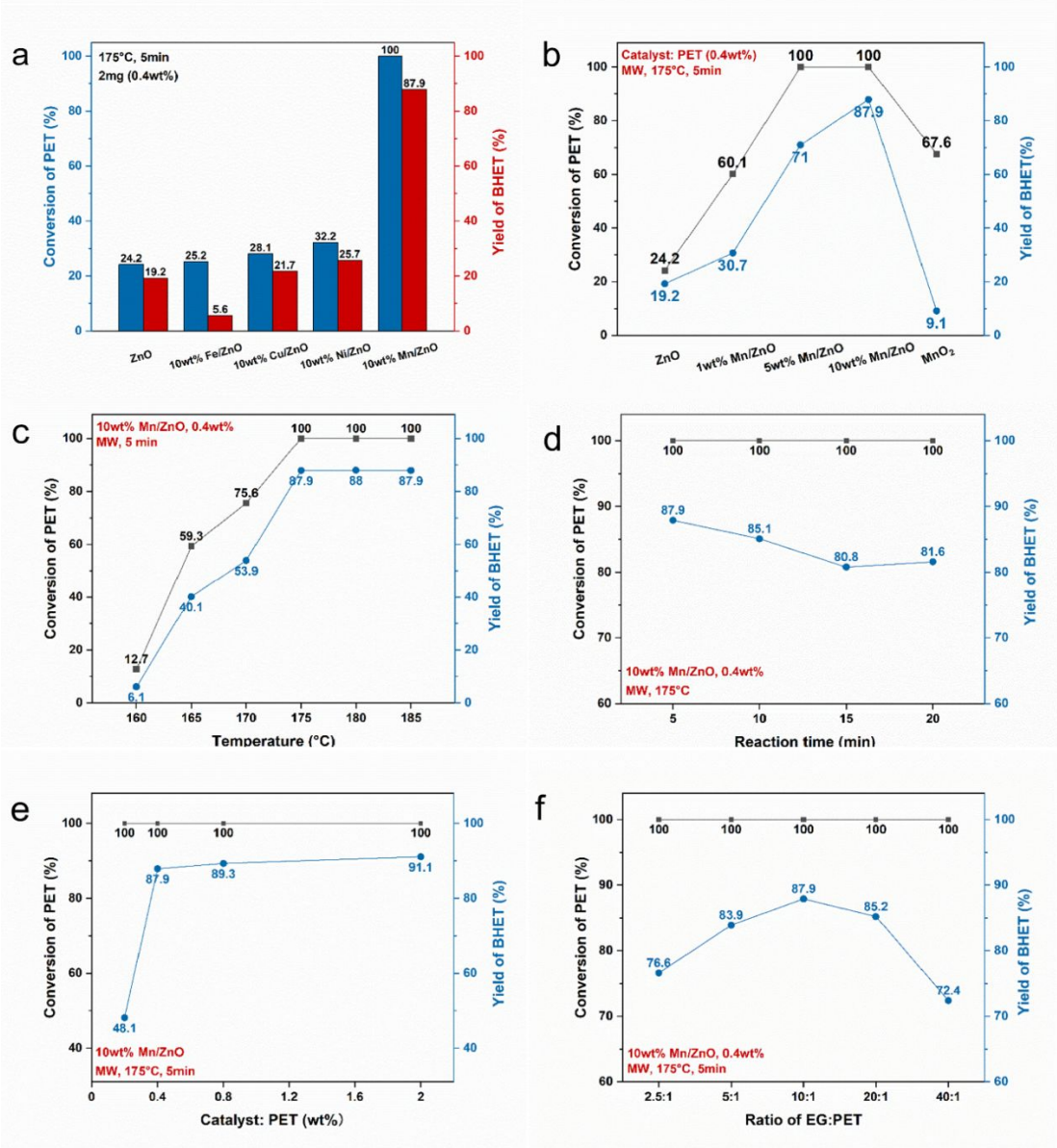

Figure 2. (a) Conversion of PET and yield of BHET with different cocatalysts on ZnO. (b) Effect of different Mn loading amounts on PET depolymerisation. (c) Effect of the reaction temperature using 10wt% Mn/ZnO. (d) Effect of the reaction time using 10wt% Mn/ZnO. (e) Effect of different ratios of 10wt% Mn/ZnO to PET. (f) Effect of different weight ratios of EG to PET.

The loading amount of Mn cocatalyst on ZnO was then studied to further improve the glycolysis of PET by microwave catalysis. The results are shown in Figure 2 (b), in which pure ZnO and MnOx were used as two references. MnOx is found to show much higher conversion of PET (67.6%) than ZnO (24.2%), but a lower yield of BHET (9.1%) compared with ZnO (19.2%). Interestingly, the catalytic performance increases with increasing loading amount of Mn cocatalyst on ZnO. The 10 wt% Mn/ZnO catalyst exhibits the best performance, i.e. 100% conversion of PET and 87.9% yield of BHET at 175°C for 5 minute reaction, indicating that Mn cocatalyst plays a significant role in the depolymerisation of PET to oligomers.

Optimisation of the reaction parameters

Reaction temperature was next investigated to optimise the reaction conditions. The temperature ranges from 160 - 185°C and the reaction time was set as 5 minutes. The results are shown in Figure 2 (c). The conversion of PET is 12.7% and the yield of BHET is 6.1% when reaction was operated at 160°C for 5 minutes. The conversion of PET and the yield of BHET increases with increasing reaction temperature, and the conversion reaches 100% at 175°C, while the yield levels off after this temperature at around 88%. Results strongly indicate that the 10 wt% Mn/ZnO exhibits good catalytic performance at this low reaction temperature. The reaction time effect is also investigated using 10wt% Mn/ZnO catalyst at 175°C. Since the ramping procedure by microwave irradiation takes around 3 minutes, the results achieved is not very reliable when the overall reaction times is below 5 minutes, so the min reaction time is set as 5 min. The reactions were performed for 5, 10, 15 and 20 minutes. The results are shown in Figure 2 (d). The conversion of PET maintains 100% with extending the reaction time from 5 minutes to 20 minutes. The yield to BHET however shows an opposite trend. It drops from 87.9% to 81.6% with increasing the reaction time from 5 to 20 minutes. It is believed that increasing the reaction time might enhance oligoerisation and shift the product from monomer BHET to its dimer or oligomers[26,27].

The ratios of the catalyst to PET plastic were changed to optimise the glycolysis of PET at 175°C for 5 minutes. The results are shown in Figure 2 (e). The conversion of PET achieves 100% even with only a small amount (0.2 wt %) of the catalyst. But the yield of BHET is found to be only 48.1%. The conversion of PET maintains 100% with increasing amount of the catalyst Mn/ZnO. The yield of BHET increases to 87.9% with the ratio of 0.4 wt% and does not show significantly increasing with further increasing the amount of the catalyst.

The weight ratio of PET to EG was also studied to further optimise the reaction condition. The results are shown in Figure 2 (f), which shows that PET is 100% degraded in the whole range of EG: PET from 2.5:1 to 40:1, while the yield of BHET shows a maximum around a ratio of 10:1. The yield of BHET increases from 76.6% to 87.9% with the weight ratio of EG: PET increasing from 2.5:1 to 10:1 and then drops up to a value of 72.4% at 40:1 ratio. This is most likely due to the highly diluted PET when the solvent amount is too high. The 10:1 weight ratio of EG:PET gives 100% conversion of PET and 87.9% yield of BHET, a superior catalytic performance reported so far.

Stability test and comparison with the conventional heating

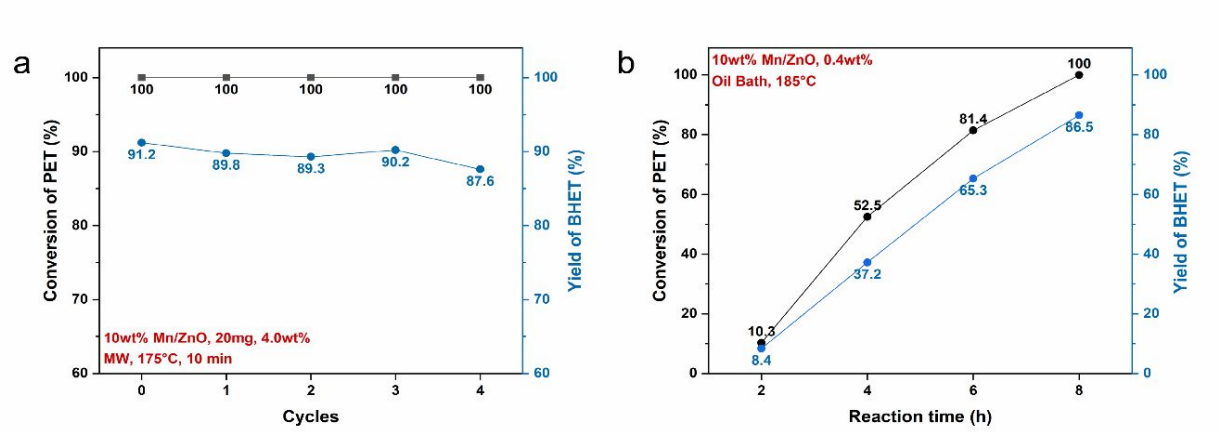

Figure 3. (a) Stability test of 10wt% Mn/ZnO for 5 cycles. (b) Conversion of PET and yield of BHET using 10wt% Mn/ZnO in an oil bath for different reaction times.

The stability of a catalyst is crucial for its application. Figure 3 (a) presents the stability of the optimised 10 wt% Mn/ZnO catalyst. The catalyst keeps 100% conversion rate of PET and shows a similar yield of BHET across 5 cycles, indicating the excellent stability of the catalyst in glycolysis of PET.

The conventional heating method was then applied with 10wt% Mn/ZnO for glycolysis of PET in order to investigate the effects of different heating methods. The reaction was operated at 185°C in the oil bath, which is 10°C higher than the temperature used in MW heating method. The results are shown in Figure 3 (b). The conversion of PET and yield of BHET increase with the reaction time, but the conversion reaches 100% only after 8 h, while the highest yield achieved at that time is 86.5%. So MW heating shortens the reaction time by a factor of 100 times. This is likely because that MW heating generates intense local heating, which can create specific hot spots on the catalyst surface[28] and enhance the reaction rate.

Characterisation of BHET

The ^{1}H NMR and ^{13}C NMR spectra were used to characterise the product BHET. DMSO-d_6 was used as a solvent, which could provide a clear sign of -OH in ^{1}H NMR spectrum. The spectra of the product formed with 10wt% Mn/ZnO at 175°C for 5 minutes are shown in Figures 4 (a) and (b), respectively. The commercial BHET (≥94.5%, Sigma-Aldrich) was used as a reference and its spectra are shown in Figures 4 (c) and (d), respectively.

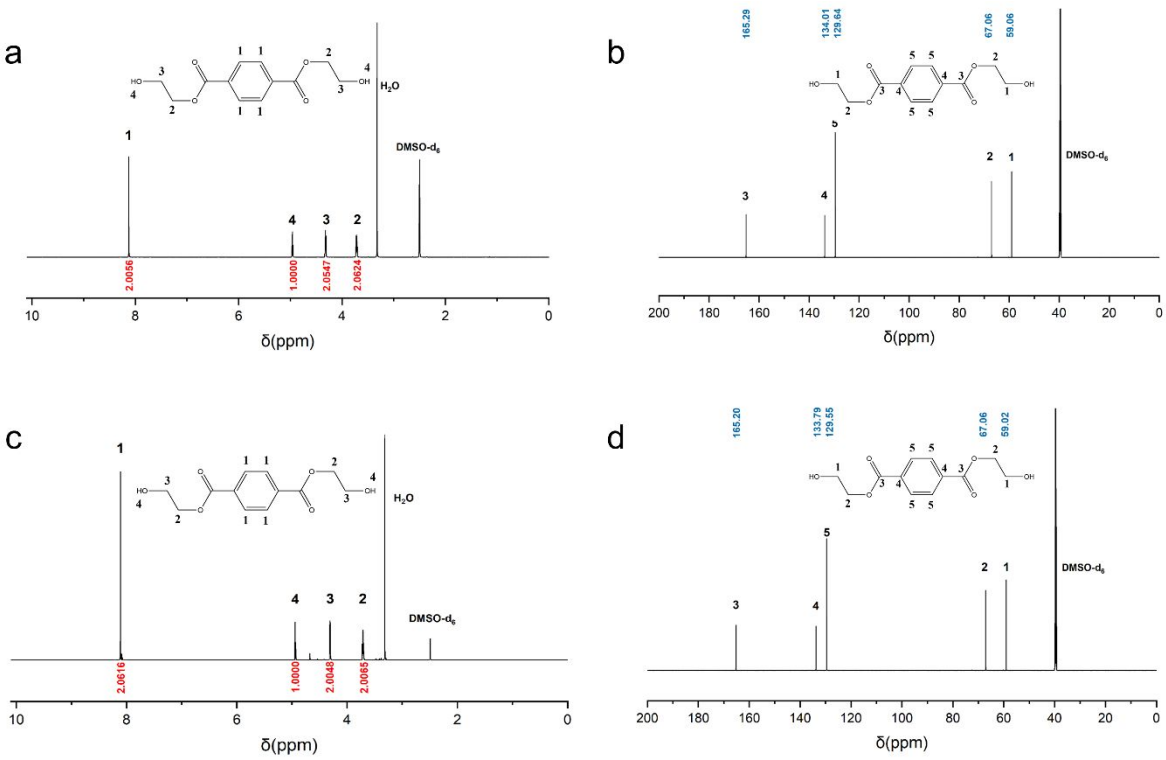

Figure 4. ^{1}H NMR spectrum (a) and ^{13}C NMR spectrum (b) of products by using 10wt% Mn/ZnO as the catalyst, operated at 175°C for 5 minutes.^{1}H NMR spectrum (c) and ^{13}C NMR spectrum (d) of the commercial BHET. The solvent is DMSO-d_6.

The signs shown in Figure 4 (a) are assigned to the protons of the aromatic ring at the following chemical shifts (δ): (δH = 8.1 ppm, 4H), hydroxyl groups (δH = 4.95 ppm, 2H), methylene (-CH_2-) adjacent to the -OH groups (δH = 3.73 ppm, 4H), methylene (-CH_2-) adjacent to the -COO groups (δH = 4.33 ppm, 4H), respectively. The sign at 3.3 ppm is attributed to H_2O residual and contamination. The signs shown in Figure 4 (b) (δC = 165.3 ppm), (δC = 134.0 ppm), (δC = 129.6 ppm), (δC = 67.1 ppm) and (δC = 59.1 ppm) are assigned to the carbons of the chemical structure of obtained BHET.

For the commercial BHET, the signs shown in Figure (c) are assigned to the protons of the aromatic ring (δH = 8.1 ppm, 4H), hydroxyl groups (δH = 4.95 ppm, 2H), methylene (-CH_2-) adjacent to the -OH groups (δH = 3.73 ppm, 4H), methylene (-CH_2-) adjacent to the -COO groups (δH = 4.33 ppm, 4H), respectively. The sign at 3.3 ppm attributed to H_2O residual and contamination. The signs shown in Figure (d) (δC = 165.2 ppm), (δC = 133.8 ppm), (δC = 129.5 ppm), (δC = 67.1 ppm) and (δC = 59.0 ppm) are assigned to the carbons of the chemical structure of the commercial BHET. So proton and carbon spectra exhibit strong similarity between the prepared BHET and commercial one, also agreement with those documented[29,30]. The observation of no other peaks in the ^{1}H and ^{13}C NMR spectra strongly suggest the high purity of the product. The BHET produced via this process could be easily separated from any side products, resulting in a high purity monomer.

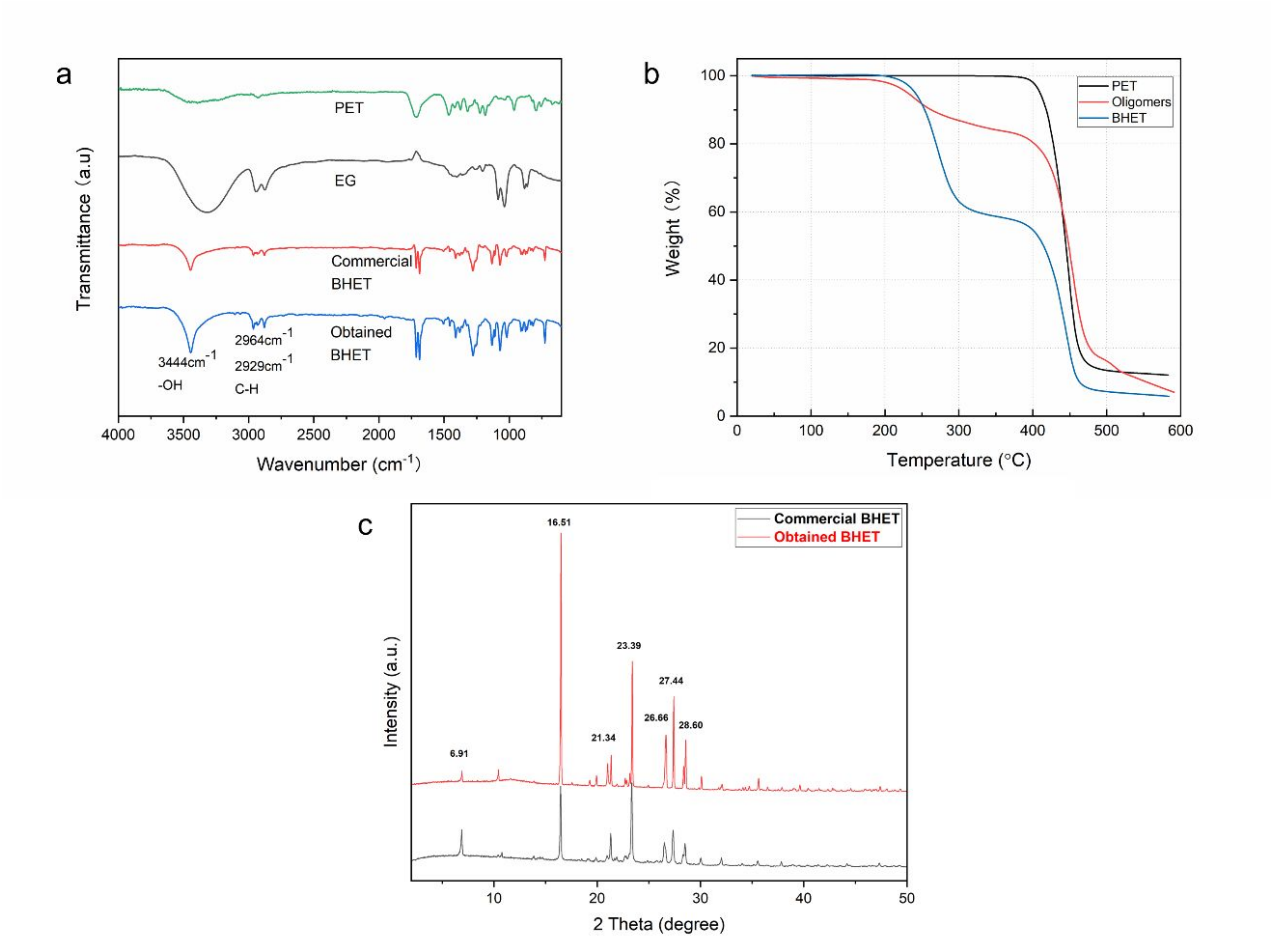

Figure 5. (a) FTIR spectra of PET, EG, commercial BHET, and BHET product obtained from the reaction. (b) TGA curves of PET, oligomers, and BHET produced from the reaction. (c) XRD spectra of commercial BHET and BHET product obtained from the reaction.

The FTIR analysis was performed on PET, EG, commercial BHET, and obtained BHET. The results are shown in Figure 5 (a). The characteristic peaks of BHET are shown at 3444, 2964, and 2929 cm^{-1}, respectively, corresponding to hydroxyl group (–OH) and alkyl group (C-H, sp^3). Other peaks appear in 1710, 1690, 1500, and 1280 cm^{-1} are identified as C=O (1710, 1690 cm^{-1}), benzene ring (1500 cm^{-1}), and C-O (1280 cm^{-1}). The above list of peaks covers all functional groups of BHET.

Figure 5(b) shows the thermogravimetric analysis of PET, as well as this of oligomers and BHET. For the sample of BHET monomers, the first mass loss starts at 203°C with the second loss of mass at 400°C corresponding to the decomposition of PET produced by re-polymerisation in the heating ramp. The first mass loss of oligomers sample was observed at 198°C, and similar second mass loss was observed at around 400°C corresponding to the decomposition of re-polymerised PET during the ramping procedure[31]. Only one mass loss was observed with pure PET at the decomposition temperature around 400°C.

The XRD spectra in Figure 5 (c) display distinct peaks at 2θ values of 6.91º, 16.51º, 21.34º, 23.39º, 26.66º, 27.44º and 28.60º, which are in good agreement with the typical peaks reported in previous studies on BHET crystals[32]. The high degree of crystallinity of the BHET product is evidenced by the sharp and well-defined peaks observed in the XRD spectra.

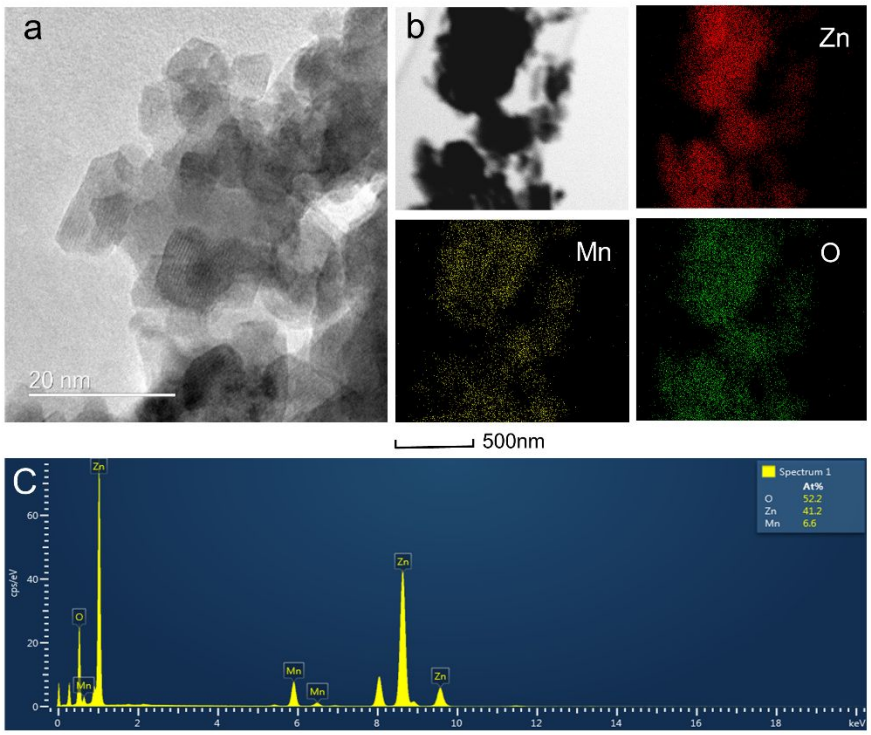

Figure 6. (a) TEM images of 10wt% Mn/ZnO. (b) EDX mapping images, (c) EDX sum spectrum of the surface of 10wt% Mn/ZnO.

The morphology of 10wt% Mn/ZnO was first investigated by TEM, as shown in Figure 6 (a). There are no obvious manganese oxide particles observed on ZnO, which might be due to highly dispersed fine MnOx particles. The particles of the catalyst typically exhibit an irregular shape with varying sizes, while EDX mapping image in Figure 6 (b) shows a homogeneous distribution of manganese oxide on ZnO. The EDX scanning shows 6.6% of manganese in the scanned area, which is close to the actual amount (10%). The irregular shape of the cocatalyst, in turn, can improve the dielectric loss properties of the material, making it more efficient for absorbing microwave irradiation[33]. By considering the outcomes of the experiment utilizing the conventional oil bath as a heating source, this can be attributed to MW rapid and selective heating of the reactants (e.g. EG) and the catalyst, leading to a higher reaction rate and enhanced formation of the desired product[34].

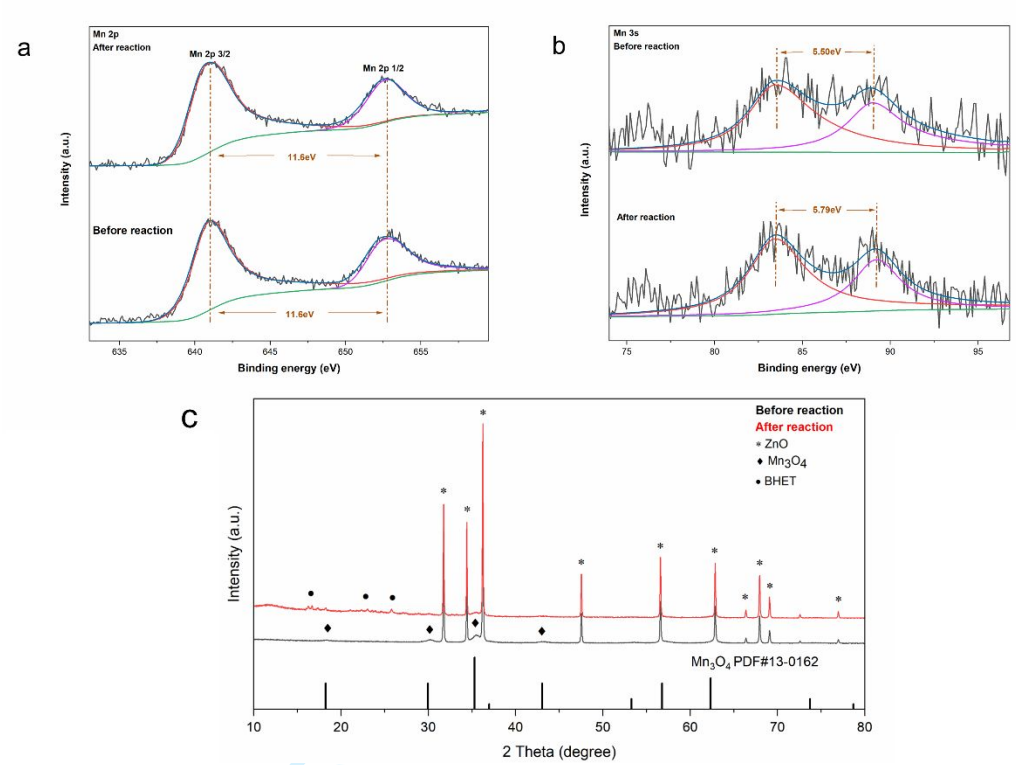

Figure 7. XPS and XRD spectra of Mn/ZnO before and after the reaction. (a) deconvolution of Mn 2p before and after reaction, (b) deconvolution of Mn 3s before and after reaction, (c) XRD spectra of 10wt% Mn/ZnO before and after reaction.

Next the element state of manganese oxide in the catalyst material was characterised by employing two complementary analytical techniques: X-ray photoelectron spectroscopy (XPS) and X-ray diffraction (XRD). Indeed, the changes in the oxidation state and coordination environment of the elements in the catalyst can provide insights into the mechanism by which the catalyst promotes the chemical reaction. By comparing the XPS and XRD spectra of the 10wt% Mn/ZnO before and after the reaction, it is possible to identify changes in the chemical environment of the active sites, which can be correlated with changes in the reaction rate. It is noted that the catalyst tested after the reaction is mixed with oligomers and BHET, which may potentially influence the electronic structure of the catalyst. This information can help elucidate the catalytic mechanism and identify the factors that contribute to the catalyst's activity.

Figure 7 (a) and (b) show the high-resolution XPS spectra of Mn 2p and Mn 3s peaks before and after the reaction, respectively. Due to the occurrence of spin orbit splitting, Mn 2p peak gives rise to a doublet with the two possible states 3/2 and 1/2 having different binding energies at 640.96 and 652.56 eV with energy splitting of 11.6 eV. Correspondingly two peaks of 83.31 and 88.81eVwith energy splitting of 5.50 eV indicate typical Mn 3s electrons before the reaction, as shown in Figure 7 (b). The XPS spectra of manganese oxide before the reaction is similar with the previous report on

XPS spectrum of Mn_3O_4[35]. The Mn_3O_4 compound exhibits a normal spinel structure, where Mn can occupy different oxidation states in the tetrahedral sites (Mn^{2+}) and octahedral sites (Mn^{3+}). The chemical composition of $Mn^{2+}[Mn^{3+}{}_2]O^{2-}{}_4$ represents the distribution of these ions in the crystal lattice[36]. After reaction, the energy splitting of the Mn 2p peaks keeps at 11.6eV, while the energy splitting of XPS spectra of the Mn 3s peaks increases from 5.5 eV to 5.79 eV during the reaction. This can be attributed to the reduction of surface Mn^{3+} species[37]. The reduction of surface Mn^{3+} to Mn^{2+} is likely to occur due to the interaction of the catalyst with the oligomers and BHET. Combined with the XRD spectra of the catalyst in Figure 7 (c), a small amount of BHET is shown on the surface of the catalyst and no significant peaks of MnO were identified, indicating that only a portion of the Mn^{3+} species is reduced to Mn^{2+} while most of the catalyst components remain as Mn_3O_4. This observation suggests that the Mn^{3+} species serve as the primary active site in the reaction and likely undergoes coordination with the reactants to form transition states, highlighting the important role of Mn^{3+} in the catalytic process.

The XRD spectra in Figure 7 (c) display distinct peaks labeled with rhombuses (♦), which are in good agreement with the standard JCPDS Card No. 00-13-0162, and confirms the presence of Mn_3O_4 loaded on ZnO. The XRD spectra of ZnO exhibits distinct peaks labeled with asterisks (*), which are in accordance with the JCPDS Card No. 00-36-1461. The XRD spectra of BHET shows distinct peaks labeled with dots (•), which are in good agreement with the typical peaks reported in previous studies on BHET crystals[32]. Notably, no significant changes were observed in the distinct peaks of the XRD spectra before and after the reaction, indicating the stability of the catalyst under the reaction conditions.

4.5 Reaction mechanism

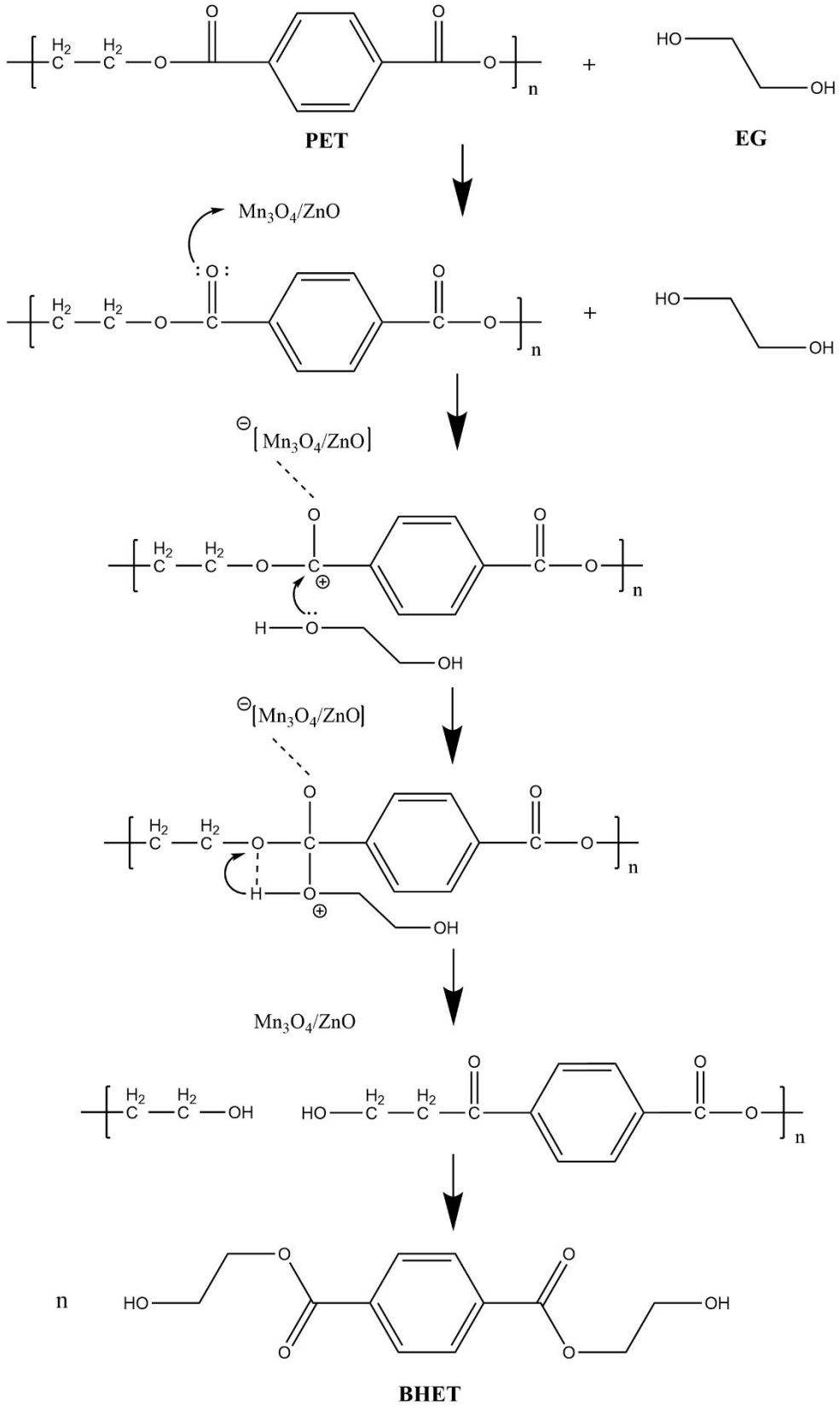

Scheme 1. The proposed mechanism of the glycolysis of PET catalysed by 10 wt% Mn/ZnO.

The observed glycolysis of PET by microwave catalysis can be attributed to the synergistic effect of Mn_3O_4 cocatalyst, ZnO catalyst, and special MW heating. The loss tangent (tanδ) is one of the most important parameters to assess the capabilities of a material to absorb microwave irradiation. The loss tangent represents the ratio of imaginary (ε″) to real (ε′) permittivity, and the material with loss tangent exceeding 0.05 is an excellent MW absorber[38]. ZnO was reported with a low loss tangent value (< 0.015 at frequency of 2.43GHz)[38]. The loss tangent of 0.026 at the frequency of 18GHz for Mn_3O_4 particles was observed in other study[39]. Despite the loss tangent of both Mn_3O_4 and ZnO particles were not reported as excellent MW absorbers, loading Mn_3O_4 on the support (reduced graphene oxide) to form nanocomposite was reported to present high loss tangent (1.10-0.67 at frequency of 2 to 18GHz)[40]. Therefore, the loss tangent of Mn_3O_4/ZnO is considered to be high. Meanwhile, the irregular shape of Mn_3O_4/ZnO nanoparticles should enhance their dielectric properties[41], resulting in more efficient heating under microwave irradiation.. Furthermore, the low concentration (10%) of Mn_3O_4 loaded onto the ZnO provides additional Lewis acid sites[42], promoting the dissociation of glycol from PET, which results in a higher conversion of PET to BHET[14,43]. The ZnO catalyst, in addition to its own catalytic activity, can also contribute to the MW-specific heating at the local area of the Mn_3O_4/ZnO, promoting the glycolysis reaction and enhancing the overall performance of the system. EG as the solvent and one reactant, can also absorb MW irradiation as it has a loss tangent of 0.8 at frequency of 2.45GHz[44].

As it is very challenging to monitor what happened in the microwave reactor due to safety reasons, we have to propose the reaction mechanism based on the catalyst characterisation before and after the reaction as well as the products formed. The scheme 1 shows the proposed mechanism of glycolysis of PET by using Mn/ZnO. Both Mn/ZnO and EG are heated by MW and transfer heat to PET which is then fast dissolved in EG at temperature of large than 170°C[45], which also interprets the low conversion of PET when the reaction temperature is below 170°C (Figure 2c) . The catalyst next acts as a Lewis acid to attract the lone electron pair in the oxygen atom of the ester group, which promotes the cleavage of the ester bond[46]. The Mn_3O_4 component of the catalyst is particularly effective in this regard due to its Lewis acidic nature[19]. The pathway for the glycolysis of PET plastic can be divided into three main steps: initiation, propagation, and termination. In the initiation step, the Mn/ZnO catalyst under MW heating activates the ester bond by attracting the lone electron pair in the oxygen atom. This results in the formation of a reactive intermediate in which the carbonyl group is protonated, and the oxygen atom becomes positively charged. This step is crucial for the subsequent propagation of the reaction. In the propagation step, the activated ester bond reacts with ethylene glycol, resulting in the formation of an intermediate cyclic structure. This structure is then reduced by the Mn/ZnO catalyst, resulting in the formation of the constituent monomers, ethylene glycol and terephthalic acid while the catalyst restores. The Mn_3O_4 component of the catalyst plays a key role in this step by promoting the cleavage of the ester bond[18]. In the termination step, the monomers are separated from the reaction mixture by distillation and recrystallization. The catalyst can be recycled and reused for subsequent glycolysis reactions.

4. Conclusion

In this work an innovative approach was utilized to directly depolymerise PET water bottle waste into its monomers BHET utilizing microwave catalysis and Mn/ZnO as a catalyst. The Mn/ZnO catalyst was found to be highly efficient in depolymerising PET into its monomers, with a mass ratio of only 0.4% catalyst to PET. The PET depolymerisation was observed to be highly dependent on various reaction parameters, such as the reaction time, temperature, and Mn/ZnO loading. The optimised conditions for maximum conversion of PET and yield towards BHET were determined to be 175°C for 5-minute run over Mn 10wt/% ZnO, resulting in 100% conversion of PET and 88% yield towards BHET, which is a record obtained at such low temperature and short reaction time.

The MW catalyst Mn/ZnO further demonstrates excellent reusability, making it a promising candidate for industrial-scale PET recycling. It is evident that there is a need for further development to enhance the sustainability of this method. Nevertheless, we believe that the present results are significant contribution to circular economy by presenting a promising solution for achieving a closed loop in recycling PET waste.

Author Contributions

The manuscript was written through the contributions of all authors. All authors have approved the final version of the manuscript.

Conflict of Interest

There is no conflict of interest to report.

Acknowledgements

Z.Y., G.M., and J.T are thankful for UK EPSRC project (EP/S018204/2) and Royal Society Leverhulme Trust Senior Research Fellowship (SRF\R1\21000153).

Author information

Authors and Affiliations

Department of Chemical Engineering, University College London, London, UK

Zhe Yuan, George Manos & Junwang Tang

Key Lab of Synthetic and Natural Functional Molecule Chemistry of Ministry of Education, The Energy and Catalysis Hub, College of Chemistry and Materials Science, Northwest University, Xi'an, P. R. China

Jianlong Yang

Industrial Catalysis Center, Department of Chemical Engineering, Tsinghua University, Beijing, China

Junwang Tang

References

(1) The Oxford Dictionary of National Biography. In *The Oxford Dictionary of National Biography*; Matthew, H. C. G., Harrison, B., Eds.; Oxford University Press: Oxford, 2004; p ref:odnb/21350. https://doi.org/10.1093/ref:odnb/21350.

(2) Geyer, R.; Jambeck, J. R.; Law, K. L. Production, Use, and Fate of All Plastics Ever Made. *Sci. Adv.* **2017**, *3* (7), e1700782. https://doi.org/10.1126/sciadv.1700782.

(3) *Microplastics in the oceans: the solutions lie on land*. https://journals.openedition.org/factsreports/5290 (accessed 2021-10-26).

(4) Plastic crisis needs binding treaty, report says. *BBC News*. January 18, 2022. https://www.bbc.com/news/science-environment-60026748 (accessed 2022-01-18).

(5) Siddiqui, M. N.; Redhwi, H. H.; Achilias, D. S. Recycling of Poly(Ethylene Terephthalate) Waste through Methanolic Pyrolysis in a Microwave Reactor. *J. Anal. Appl. Pyrolysis* **2012**, *98*, 214–220. https://doi.org/10.1016/j.jaap.2012.09.007.

(6) Raheem, A. B.; Noor, Z. Z.; Hassan, A.; Abd Hamid, M. K.; Samsudin, S. A.; Sabeen, A. H. Current Developments in Chemical Recycling of Post-Consumer Polyethylene Terephthalate Wastes for New Materials Production: A Review. *J. Clean. Prod.* **2019**, *225*, 1052–1064. https://doi.org/10.1016/j.jclepro.2019.04.019.

(7) Shamsaei, M.; Aghayan, I.; Kazemi, K. A. Experimental Investigation of Using Cross-Linked Polyethylene Waste as Aggregate in Roller Compacted Concrete Pavement. *J. Clean. Prod.* **2017**, *165*, 290–297. https://doi.org/10.1016/j.jclepro.2017.07.109.

(8) Yoshioka, T.; Sato, T.; Okuwaki, A. Hydrolysis of Waste PET by Sulfuric Acid at 150°C for a Chemical Recycling. *J. Appl. Polym. Sci.* **1994**, *52* (9), 1353–1355. https://doi.org/10.1002/app.1994.070520919.

(9) Paszun, D.; Spychaj, T. Chemical Recycling of Poly(Ethylene Terephthalate). *Ind. Eng. Chem. Res.* **1997**, *36* (4), 1373–1383. https://doi.org/10.1021/ie960563c.

(10) Al-Sabagh, A. M.; Yehia, F. Z.; Eshaq, Gh.; Rabie, A. M.; ElMetwally, A. E. Greener Routes for Recycling of Polyethylene Terephthalate. *Egypt. J. Pet.* **2016**, *25* (1), 53–64. https://doi.org/10.1016/j.ejpe.2015.03.001.

(11) Genta, M.; Iwaya, T.; Sasaki, M.; Goto, M.; Hirose, T. Depolymerization Mechanism of Poly(Ethylene Terephthalate) in Supercritical Methanol. *Ind. Eng. Chem. Res.* **2005**, *44* (11), 3894–3900. https://doi.org/10.1021/ie0488187.

(12) Yang, Y.; Lu, Y.; Xiang, H.; Xu, Y.; Li, Y. Study on Methanolytic Depolymerization of PET with Supercritical Methanol for Chemical Recycling. *Polym. Degrad. Stab.* **2002**, *75* (1), 185–191. https://doi.org/10.1016/S0141-3910(01)00217-8.

(13) Barnard, E.; Arias, J. J. R.; Thielemans, W. Chemolytic Depolymerisation of PET: A Review. *Green Chem.* **2021**, *23* (11), 3765–3789. https://doi.org/10.1039/D1GC00887K.

(14) López-Fonseca, R.; Duque-Ingunza, I.; de Rivas, B.; Arnaiz, S.; Gutiérrez-Ortiz, J. I. Chemical Recycling of Post-Consumer PET Wastes by Glycolysis in the Presence of Metal Salts. *Polym. Degrad. Stab.* **2010**, *95* (6), 1022–1028.

https://doi.org/10.1016/j.polymdegradstab.2010.03.007.

(15) Baliga, S.; Wong, W. T. Depolymerization of Poly(Ethylene Terephthalate) Recycled from Post-Consumer Soft-Drink Bottles. *J. Polym. Sci. Part Polym. Chem.* **1989**, *27* (6), 2071–2082. https://doi.org/10.1002/pola.1989.080270625.

(16) López-Fonseca, R.; Duque-Ingunza, I.; de Rivas, B.; Flores-Giraldo, L.; Gutiérrez-Ortiz, J. I. Kinetics of Catalytic Glycolysis of PET Wastes with Sodium Carbonate. *Chem. Eng. J.* **2011**, *168* (1), 312–320. https://doi.org/10.1016/j.cej.2011.01.031.

(17) Shukla, S. R.; Harad, A. M. Glycolysis of Polyethylene Terephthalate Waste Fibers. *J. Appl. Polym. Sci.* **2005**, *97* (2), 513–517. https://doi.org/10.1002/app.21769.

(18) M. Al-Sabagh, A.; Z. Yehia, F.; K. Harding, D. R.; Eshaq, G.; E. ElMetwally, A. Fe 3 O 4 -Boosted MWCNT as an Efficient Sustainable Catalyst for PET Glycolysis. *Green Chem.* **2016**, *18* (14), 3997–4003. https://doi.org/10.1039/C6GC00534A.

(19) Zhang, H.; Gao, Q.; Li, Z.; Xu, P.; Xiao, H.; Zhang, T.; Liang, X. A RGO-Based Fe2O3 and Mn3O4 Binary Crystals Nanocomposite Additive for High Performance Li–S Battery. *Electrochimica Acta* **2020**, *343*, 136079. https://doi.org/10.1016/j.electacta.2020.136079.

(20) Imran, M.; Kim, D. H.; Al-Masry, W. A.; Mahmood, A.; Hassan, A.; Haider, S.; Ramay, S. M. Manganese-, Cobalt-, and Zinc-Based Mixed-Oxide Spinels as Novel Catalysts for the Chemical Recycling of Poly(Ethylene Terephthalate) via Glycolysis. *Polym. Degrad. Stab.* **2013**, *98* (4), 904–915. https://doi.org/10.1016/j.polymdegradstab.2013.01.007.

(21) Eshaq, Gh.; ElMetwally, A. E. (Mg–Zn)–Al Layered Double Hydroxide as a Regenerable Catalyst for the Catalytic Glycolysis of Polyethylene Terephthalate. *J. Mol. Liq.* **2016**, *214*, 1–6. https://doi.org/10.1016/j.molliq.2015.11.049.

(22) Pingale, N.; Shukla, S. Microwave Assisted Ecofriendly Recycling of Poly (Ethylene Terephthalate) Bottle Waste. *Eur. Polym. J.* **2008**, *44*, 4151. https://doi.org/10.1016/j.eurpolymj.2008.09.019.

(23) Chaudhary, S.; Surekha, P.; Kumar, D.; Rajagopal, C.; Roy, P. K. Microwave Assisted Glycolysis of Poly(Ethylene Terepthalate) for Preparation of Polyester Polyols. *J. Appl. Polym. Sci.* **2013**, *129* (5), 2779–2788. https://doi.org/10.1002/app.38970.

(24) Chen, F.; Wang, G.; Shi, C.; Zhang, Y.; Zhang, L.; Li, W.; Yang, F. Kinetics of Glycolysis of Poly(Ethylene Terephthalate) Under Microwave Irradiation. *J. Appl. Polym. Sci.* **2013**, *127*. https://doi.org/10.1002/app.37608.

(25) Qi, J.; Hu, X. The Loss of ZnO as the Support for Metal Catalysts by H 2 Reduction. *Phys. Chem. Chem. Phys.* **2020**, *22* (7), 3953–3958. https://doi.org/10.1039/C9CP06093F.

(26) Wang, Q.; Yao, X.; Tang, S.; Lu, X.; Zhang, X.; Zhang, S. Urea as an Efficient and Reusable Catalyst for the Glycolysis of Poly(Ethylene Terephthalate) Wastes and the Role of Hydrogen Bond in This Process. *Green Chem.* **2012**, *14* (9), 2559–2566. https://doi.org/10.1039/C2GC35696A.

(27) Wang, Q.; Yao, X.; Geng, Y.; Zhou, Q.; Lu, X.; Zhang, S. Deep Eutectic Solvents as Highly Active Catalysts for the Fast and Mild Glycolysis of Poly(Ethylene Terephthalate)(PET). *Green Chem.* **2015**, *17* (4), 2473–2479.

https://doi.org/10.1039/C4GC02401J.

(28) Galema, S. A. Microwave Chemistry. *Chem. Soc. Rev.* **1997**, *26* (3), 233–238. https://doi.org/10.1039/CS9972600233.

(29) Xi, G.; Lu, M.; Sun, C. Study on Depolymerization of Waste Polyethylene Terephthalate into Monomer of Bis(2-Hydroxyethyl Terephthalate). *Polym. Degrad. Stab.* **2005**, *87* (1), 117–120. https://doi.org/10.1016/j.polymdegradstab.2004.07.017.

(30) Imran, M.; Kim, B.-K.; Han, M.; Cho, B. G.; Kim, D. H. Sub- and Supercritical Glycolysis of Polyethylene Terephthalate (PET) into the Monomer Bis(2-Hydroxyethyl) Terephthalate (BHET). *Polym. Degrad. Stab.* **2010**, *95* (9), 1686–1693. https://doi.org/10.1016/j.polymdegradstab.2010.05.026.

(31) Chen, C.-H. Study of Glycolysis of Poly(Ethylene Terephthalate) Recycled from Postconsumer Soft-Drink Bottles. III. Further Investigation. *J. Appl. Polym. Sci.* **2003**, *87* (12), 2004–2010. https://doi.org/10.1002/app.11694.

(32) Castaño, V. M.; Alvarez-Castillo, A.; Vázquez-Polo, G.; Acosta, D.; González, V. High Resolution Electron Microscopy of Bis-(-2-Hydroxyethyl) Terephthalate Crystalline Polymers. *Microsc. Res. Tech.* **1998**, *40* (1), 41–48. https://doi.org/10.1002/(SICI)1097-0029(19980101)40:1<41::AID-JEMT6>3.0.CO;2-#.

(33) Xie, X.; Wang, B.; Wang, Y.; Ni, C.; Sun, X.; Du, W. Spinel Structured MFe2O4 (M = Fe, Co, Ni, Mn, Zn) and Their Composites for Microwave Absorption: A Review. *Chem. Eng. J.* **2022**, *428*, 131160. https://doi.org/10.1016/j.cej.2021.131160.

(34) Jie, X.; Li, W.; Slocombe, D.; Gao, Y.; Banerjee, I.; Gonzalez-Cortes, S.; Yao, B.; AlMegren, H.; Alshihri, S.; Dilworth, J.; Thomas, J.; Xiao, T.; Edwards, P. Microwave-Initiated Catalytic Deconstruction of Plastic Waste into Hydrogen and High-Value Carbons. *Nat. Catal.* **2020**, *3* (11), 902–912. https://doi.org/10.1038/s41929-020-00518-5.

(35) Jiang, H.; Zhao, T.; Yan, C.; Ma, J.; Li, C. Hydrothermal Synthesis of Novel Mn3O4 Nano-Octahedrons with Enhanced Supercapacitors Performances. *Nanoscale* **2010**, *2* (10), 2195–2198. https://doi.org/10.1039/C0NR00257G.

(36) Ramírez, A.; Hillebrand, P.; Stellmach, D.; May, M. M.; Bogdanoff, P.; Fiechter, S. Evaluation of MnO_x, Mn_2O_3, and Mn_3O_4 Electrodeposited Films for the Oxygen Evolution Reaction of Water. *J. Phys. Chem. C* **2014**, *118* (26), 14073–14081. https://doi.org/10.1021/jp500939d.

(37) Biesinger, M. C.; Payne, B. P.; Grosvenor, A. P.; Lau, L. W. M.; Gerson, A. R.; Smart, R. St. C. Resolving Surface Chemical States in XPS Analysis of First Row Transition Metals, Oxides and Hydroxides: Cr, Mn, Fe, Co and Ni. *Appl. Surf. Sci.* **2011**, *257* (7), 2717–2730. https://doi.org/10.1016/j.apsusc.2010.10.051.

(38) Omran, M.; Fabritius, T.; Heikkinen, E.-P.; Chen, G. Dielectric Properties and Carbothermic Reduction of Zinc Oxide and Zinc Ferrite by Microwave Heating. *R. Soc. Open Sci.* **2017**, *4* (9), 170710. https://doi.org/10.1098/rsos.170710.

(39) Department of Physics, Noorul Islam centre for Higher Education, Kumaracoil, Tamil Nadu 629180, India.; Rani*, C. S.; John, N. J.; Department of Physics,

Kamarajar Government Arts and Science College, Surandai, Tamil Nadu - 627 859, India. Effect of Mn3O4 on the Dielectric Characteristics of Cdo - Mn3O4 Nanocomposites. *Int. J. Innov. Technol. Explor. Eng.* **2019**, *8* (11), 1285–1292. https://doi.org/10.35940/ijitee.J9502.0981119.

(40) Wang, Y.; Guan, H.; Dong, C.; Xiao, X.; Du, S.; Wang, Y. Reduced Graphene Oxide (RGO)/Mn3O4 Nanocomposites for Dielectric Loss Properties and Electromagnetic Interference Shielding Effectiveness at High Frequency. *Ceram. Int.* **2016**, *42* (1, Part A), 936–942. https://doi.org/10.1016/j.ceramint.2015.09.022.

(41) Kum-onsa, P.; Phromviyo, N.; Thongbai, P. Suppressing Loss Tangent with Significantly Enhanced Dielectric Permittivity of Poly(Vinylidene Fluoride) by Filling with Au–Na1/2Y1/2Cu3Ti4O12 Hybrid Particles. *RSC Adv. 10* (66), 40442–40449. https://doi.org/10.1039/d0ra06980a.

(42) Zhao, L.; Chen, Z.; Zhang, P.; Zhang, Y. Improved NO Reduction by Using Metal–Organic Framework Derived MnO_x–ZnO. *RSC Adv.* **2020**, *10* (53), 31780–31787. https://doi.org/10.1039/D0RA04161K.

(43) Shao, Z.; Zhang, H. Combining Transition Metal Catalysis and Organocatalysis: A Broad New Concept for Catalysis. *Chem. Soc. Rev.* **2009**, *38* (9), 2745–2755. https://doi.org/10.1039/B901258N.

(44) Sengwa, R. J. A Comparative Dielectric Study of Ethylene Glycol and Propylene Glycol at Different Temperatures. *J. Mol. Liq.* **2003**, *108* (1), 47–60. https://doi.org/10.1016/S0167-7322(03)00173-9.

(45) Güçlü, G.; Yalçınyuva, T.; Özgümüş, S.; Orbay, M. Simultaneous Glycolysis and Hydrolysis of Polyethylene Terephthalate and Characterization of Products by Differential Scanning Calorimetry. *Polymer* **2003**, *44* (25), 7609–7616. https://doi.org/10.1016/j.polymer.2003.09.062.

(46) Al-Sabagh, A. M.; Yehia, F. Z.; Eissa, A.-M. M. F.; Moustafa, M. E.; Eshaq, G.; Rabie, A.-R. M.; ElMetwally, A. E. Glycolysis of Poly(Ethylene Terephthalate) Catalyzed by the Lewis Base Ionic Liquid [Bmim][OAc]. *Ind. Eng. Chem. Res.* **2014**, *53* (48), 18443–18451. https://doi.org/10.1021/ie503677w.

Supporting information

Microwave catalytic depolymerisation of PET plastic via glycolysis

Zhe Yuan[1], Jianlong Yang[2], George Manos[1], Junwang Tang[1,3,*]

[1]Department of Chemical Engineering, University College London, London WC1E 7JE, UK

[2]Key Lab of Synthetic and Natural Functional Molecule Chemistry of Ministry of Education, The Energy and Catalysis Hub, College of Chemistry and Materials Science, Northwest University, Xi'an, P. R. China

[3]Industrial Catalysis Center, Department of Chemical Engineering, Tsinghua University, Beijing, China

[*]Corresponding author: Junwang Tang, Email: junwang.tang@ucl.ac.uk

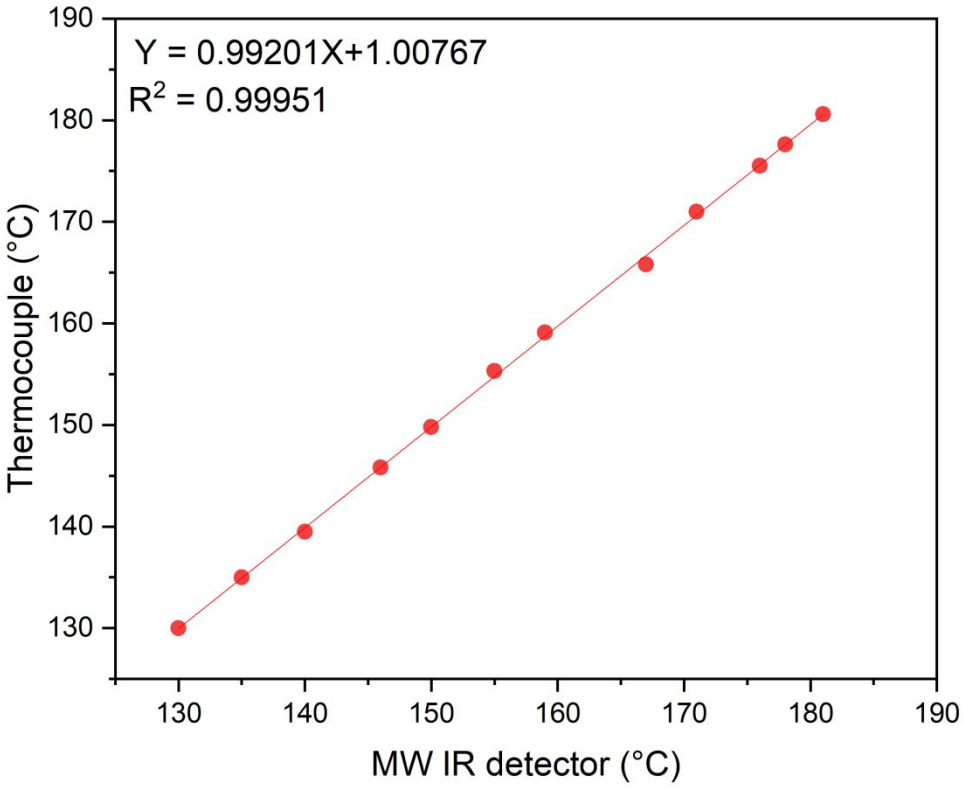

Figure S1. Calibration of MW IR temperature detector

The IR temperature detector was calibrated using a thermocouple. Ethylene glycol (EG) was used as the standard solvent for calibration. To avoid the effects of microwaves, the EG was heated to near 190°C, and then the microwave was turned off. The temperature was simultaneously recorded by both detectors during the cooling down stage, as the thermocouple was directly inserted into the EG. The results are shown in Figure S1, which indicate the accuracy of the IR temperature detector.

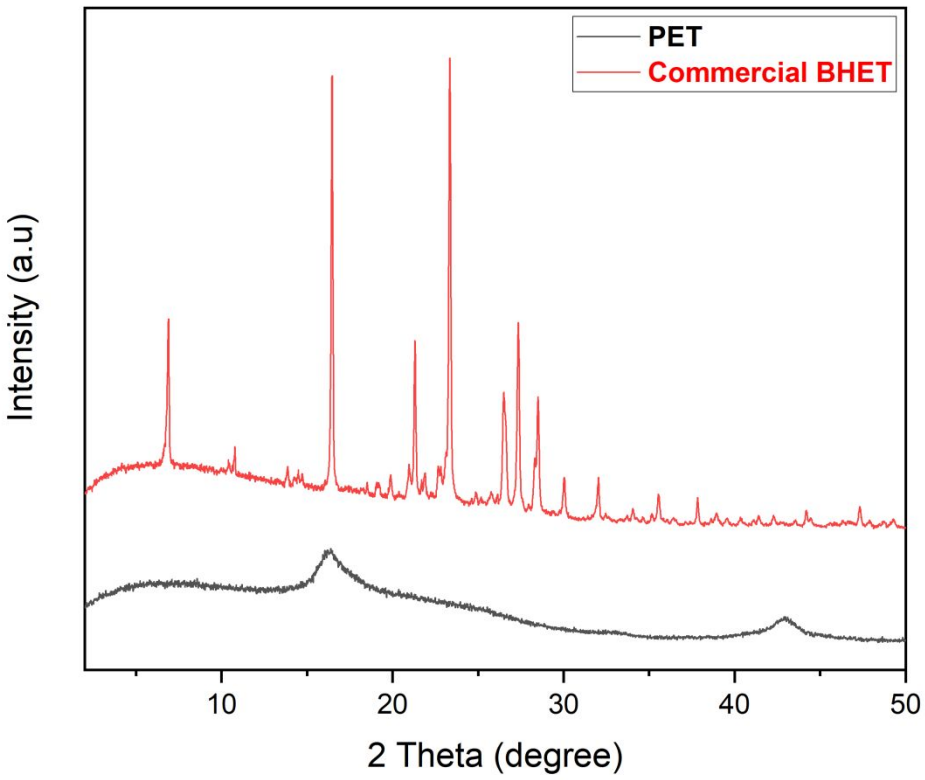

Figure S2. XRD spectra of PET and commercial BHET.

Figure S2 shows the comparison of the XRD spectra of commercial BHET and PET chips. The crystallization structure of this polyester is evidenced by the typical diffraction peaks exhibited by PET, with broader peaks observed at 16.4 and 42.9. The narrower diffraction peaks and higher relative intensity observed in BHET, in contrast to PET, indicate a distinct crystalline structure for BHET.

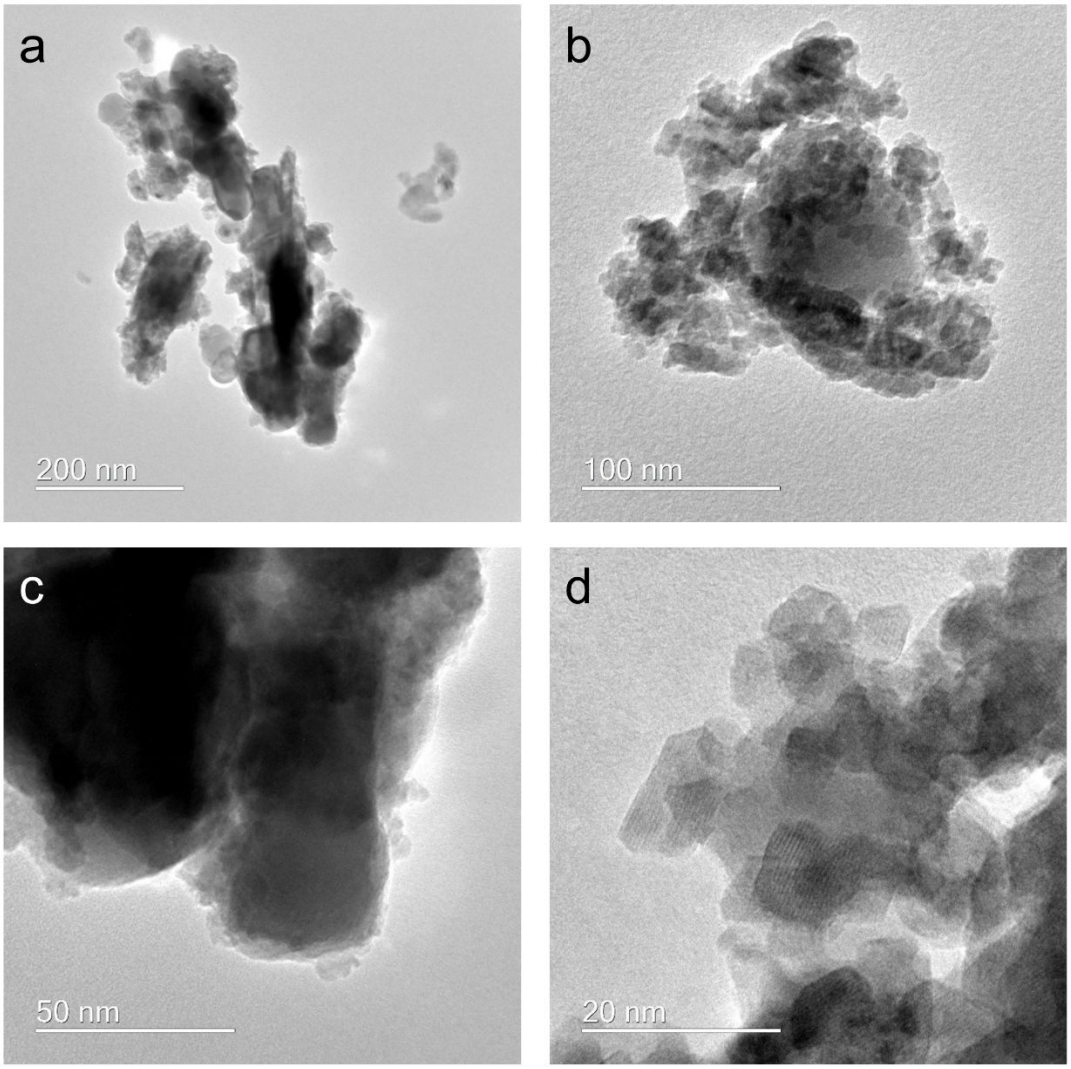

Figure S3. TEM images of 10wt% Mn/ZnO with different scales. (a) 200 nm. (b) 100nm. (c) 50nm. (d) 20nm.

Table S1. Comparison of several previously reported catalysts

No	Catalyst	Catalyst amount (mass or mole ratio,%)	Temperature (°C)	Time (min)	Conversion (%)	Yield (%)	Ref.
1	10wt% Mn/ZnO	0.4wt%	175	5	100	87.9	This work
2	$Zn(Ace)_2$	1 mol%	196	60	100	70	(1)
3	Urea	10 wt%	180	180	100	78	(2)
4	Na_2CO_3	1 mol%	196	60	100	80	(3)
5	Mg-Al hydrotalcites	1 wt%	196	50	100	81.3	(4)
6	γ-Fe_2O_3	5 wt%	300	60	100	>90	(5)
7	Fe_3O_4-boosted MWCNT	5 wt%	190	120	100	100	(6)
8	POMs	0.018 mol%	190	40	100	84.5	(7)
9	[Bmim]OH	5 wt%	190	120	100	71.2	(8)
10	$[Bmim]_2[CoCl_4]$	20 wt%	175	90	100	81.1	(9)
11	$[Bmim]FeCl_4$	20 wt%	178	240	100	59.2	(10)
12	[Bmim]Cl	80 wt%	180	480	70.1	41.6	(11)
13	[Ch][Ace]	5 wt%	180	240	100	85.2	(12)
14	GO-Mn_3O_4	1 wt%	300 (1.1MPa)	80	100	96	(13)
15	$ZnMn_2O_4$	1 wt%	260 (5MPa)	60	100	92.2	(14)
16	Ultrasmall Cobalt nanoparticles	1.5 wt%	180	180	96	77	(15)

Table S2. Real percentage of Mn over TiO_2 detected by ICP-AES

Sample	Designed	Detected (ICP-AES)
10 wt% Mn/ZnO	10	10.10

References

(1) López-Fonseca, R.; Duque-Ingunza, I.; de Rivas, B.; Arnaiz, S.; Gutiérrez-Ortiz, J. I. Chemical Recycling of Post-Consumer PET Wastes by Glycolysis in the Presence of Metal Salts. *Polymer Degradation and Stability* **2010**, *95* (6), 1022–1028. https://doi.org/10.1016/j.polymdegradstab.2010.03.007.

(2) Wang, Q.; Yao, X.; Tang, S.; Lu, X.; Zhang, X.; Zhang, S. Urea as an Efficient and Reusable Catalyst for the Glycolysis of Poly(Ethylene Terephthalate) Wastes and the Role of Hydrogen Bond in This Process. *Green Chem.* **2012**, *14* (9), 2559–2566. https://doi.org/10.1039/C2GC35696A.

(3) López-Fonseca, R.; Duque-Ingunza, I.; de Rivas, B.; Flores-Giraldo, L.; Gutiérrez-Ortiz, J. I. Kinetics of Catalytic Glycolysis of PET Wastes with Sodium Carbonate. *Chemical Engineering Journal* **2011**, *168* (1), 312–320. https://doi.org/10.1016/j.cej.2011.01.031.

(4) Chen, F.; Wang, G.; Li, W.; Yang, F. Glycolysis of Poly(Ethylene Terephthalate) over Mg–Al Mixed Oxides Catalysts Derived from Hydrotalcites. *Ind. Eng. Chem. Res.* **2013**, *52* (2), 565–571. https://doi.org/10.1021/ie302091j.

(5) Bartolome, L.; Imran, M.; Lee, K. G.; Sangalang, A.; Ahn, J. K.; Kim, D. H. Superparamagnetic γ-Fe2O3 Nanoparticles as an Easily Recoverable Catalyst for the Chemical Recycling of PET. *Green Chem.* **2013**, *16* (1), 279–286. https://doi.org/10.1039/C3GC41834K.

(6) Al-Sabagh, A. M.; Yehia, F. Z.; Harding, D. R. K.; Eshaq, G.; ElMetwally, A. E. Fe3O4-Boosted MWCNT as an Efficient Sustainable Catalyst for PET Glycolysis. *Green Chem.* **2016**, *18* (14), 3997–4003. https://doi.org/10.1039/C6GC00534A.

(7) Fang, P.; Liu, B.; Xu, J.; Zhou, Q.; Zhang, S.; Ma, J.; lu, X. High-Efficiency Glycolysis of Poly(Ethylene Terephthalate) by Sandwich-Structure Polyoxometalate Catalyst with Two Active Sites. *Polymer Degradation and Stability* **2018**, *156*, 22–31. https://doi.org/10.1016/j.polymdegradstab.2018.07.004.

(8) Yue, Q. F.; Wang, C. X.; Zhang, L. N.; Ni, Y.; Jin, Y. X. Glycolysis of Poly(Ethylene Terephthalate) (PET) Using Basic Ionic Liquids as Catalysts. *Polymer Degradation and Stability* **2011**, *96* (4), 399–403. https://doi.org/10.1016/j.polymdegradstab.2010.12.020.

(9) Wang, Q.; Geng, Y.; Lu, X.; Zhang, S. First-Row Transition Metal-Containing Ionic Liquids as Highly Active Catalysts for the Glycolysis of Poly(Ethylene Terephthalate) (PET). *ACS Sustainable Chem. Eng.* **2015**, *3* (2), 340–348. https://doi.org/10.1021/sc5007522.

(10) Wang, H.; Yan, R.; Li, Z.; Zhang, X.; Zhang, S. Fe-Containing Magnetic Ionic Liquid as an Effective Catalyst for the Glycolysis of Poly(Ethylene Terephthalate). *Catalysis Communications* **2010**, *11* (8), 763–767. https://doi.org/10.1016/j.catcom.2010.02.011.

(11) Wang, H.; Liu, Y.; Li, Z.; Zhang, X.; Zhang, S.; Zhang, Y. Glycolysis of Poly(Ethylene Terephthalate) Catalyzed by Ionic Liquids. *European Polymer Journal* **2009**, *45* (5), 1535–1544. https://doi.org/10.1016/j.eurpolymj.2009.01.025.

(12) Liu, Y.; Yao, X.; Yao, H.; Zhou, Q.; Xin, J.; Lu, X.; Zhang, S. Degradation of Poly(Ethylene Terephthalate) Catalyzed by Metal-Free Choline-Based Ionic Liquids. *Green Chem.* **2020**, *22* (10), 3122–3131. https://doi.org/10.1039/D0GC00327A.

(13) Park, G.; Bartolome, L.; Lee, K. G.; Lee, S. J.; Kim, D. H.; Park, T. J. One-Step Sonochemical Synthesis of a Graphene Oxide–Manganese Oxide Nanocomposite for Catalytic Glycolysis of Poly(Ethylene Terephthalate). *Nanoscale* **2012**, *4* (13), 3879–3885. https://doi.org/10.1039/C2NR30168G.

(14) Imran, M.; Kim, D. H.; Al-Masry, W. A.; Mahmood, A.; Hassan, A.; Haider, S.; Ramay, S. M. Manganese-, Cobalt-, and Zinc-Based Mixed-Oxide Spinels as Novel Catalysts for the Chemical Recycling of Poly(Ethylene Terephthalate) via Glycolysis. *Polymer*

Degradation and Stability **2013**, *98* (4), 904–915. https://doi.org/10.1016/j.polymdegradstab.2013.01.007.

(15) Veregue, F. R.; Pereira da Silva, C. T.; Moisés, M. P.; Meneguin, J. G.; Guilherme, M. R.; Arroyo, P. A.; Favaro, S. L.; Radovanovic, E.; Girotto, E. M.; Rinaldi, A. W. Ultrasmall Cobalt Nanoparticles as a Catalyst for PET Glycolysis: A Green Protocol for Pure Hydroxyethyl Terephthalate Precipitation without Water. *ACS Sustainable Chem. Eng.* **2018**, *6* (9), 12017–12024. https://doi.org/10.1021/acssuschemeng.8b02294.

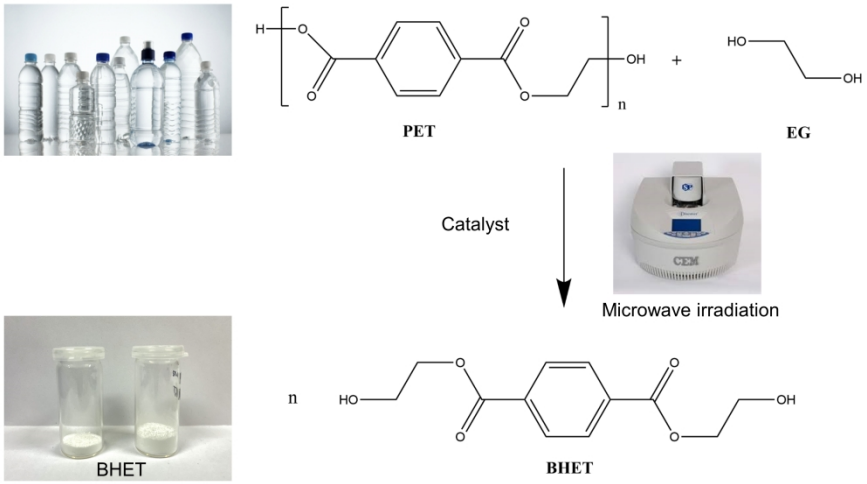

The general procedure of PET glycolysis

338x190mm (300 x 300 DPI)

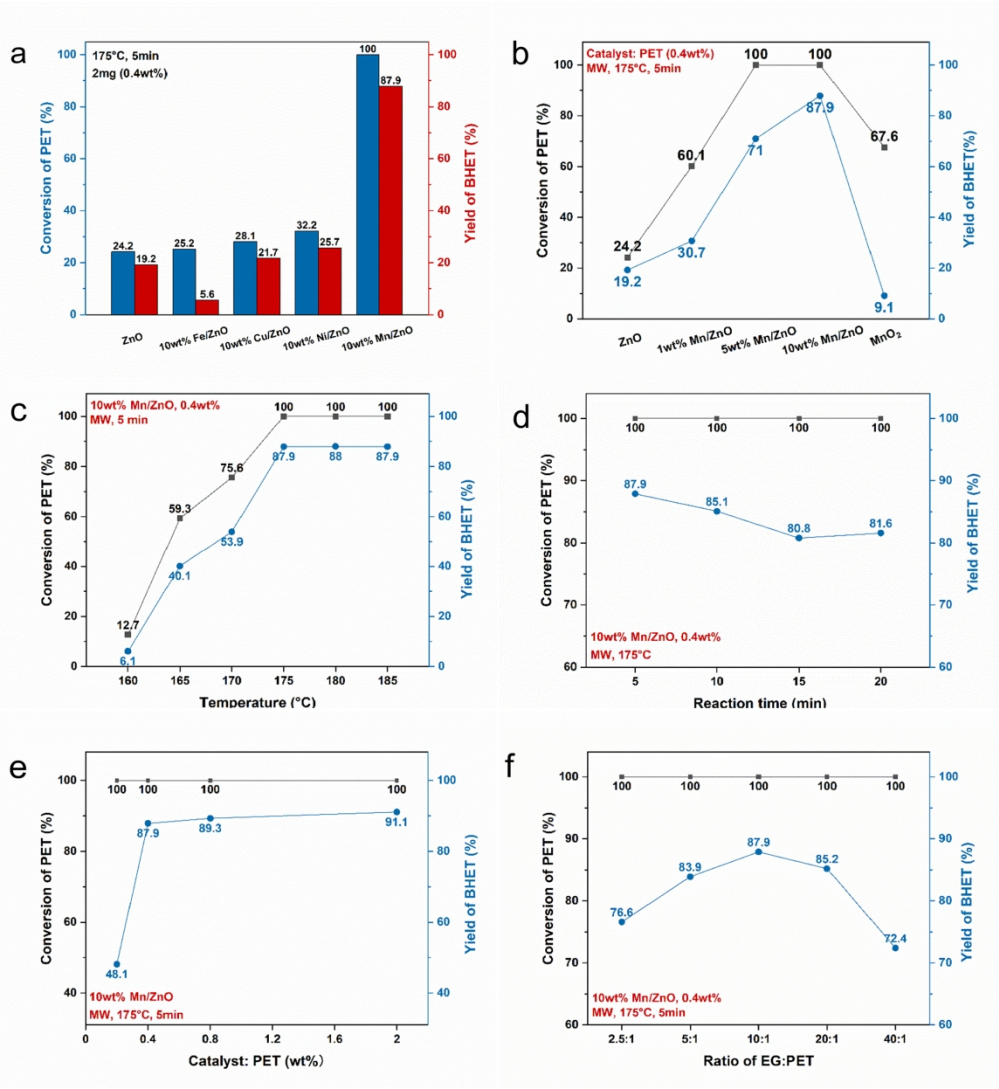

(a) Conversion of PET and yield of BHET with different cocatalysts on ZnO. (b) Effect of different Mn loading amounts on PET depolymerisation. (c) Effect of the reaction temperature using 10wt% Mn/ZnO. (d) Effect of the reaction time using 10wt% Mn/ZnO. (e) Effect of different ratios of 10wt% Mn/ZnO to PET. (f) Effect of different weight ratios of EG to PET.

192x212mm (300 x 300 DPI)

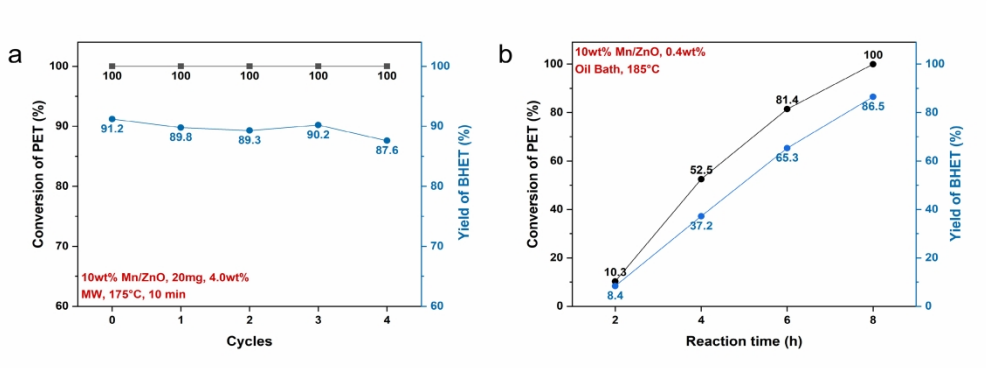

(a) Stability test of 10wt% Mn/ZnO for 5 cycles. (b) Conversion of PET and yield of BHET using 10wt% Mn/ZnO in an oil bath for different reaction times.

314x131mm (300 x 300 DPI)

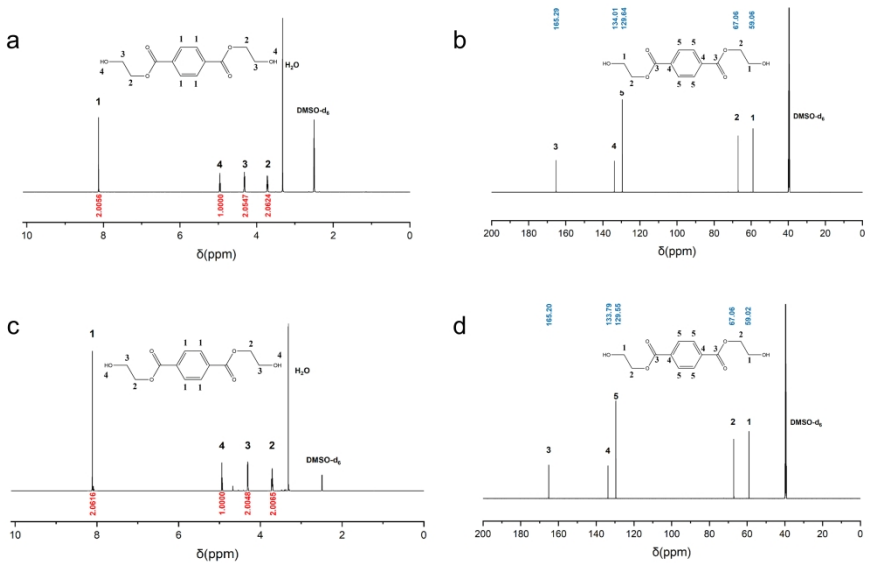

1H NMR spectrum (a) and 13C NMR spectrum (b) of products by using 10wt% Mn/ZnO as the catalyst, operated at 175°C for 5 minutes.1H NMR spectrum (c) and 13C NMR spectrum (d) of the commercial BHET. The solvent is DMSO-d6.

338x190mm (300 x 300 DPI)

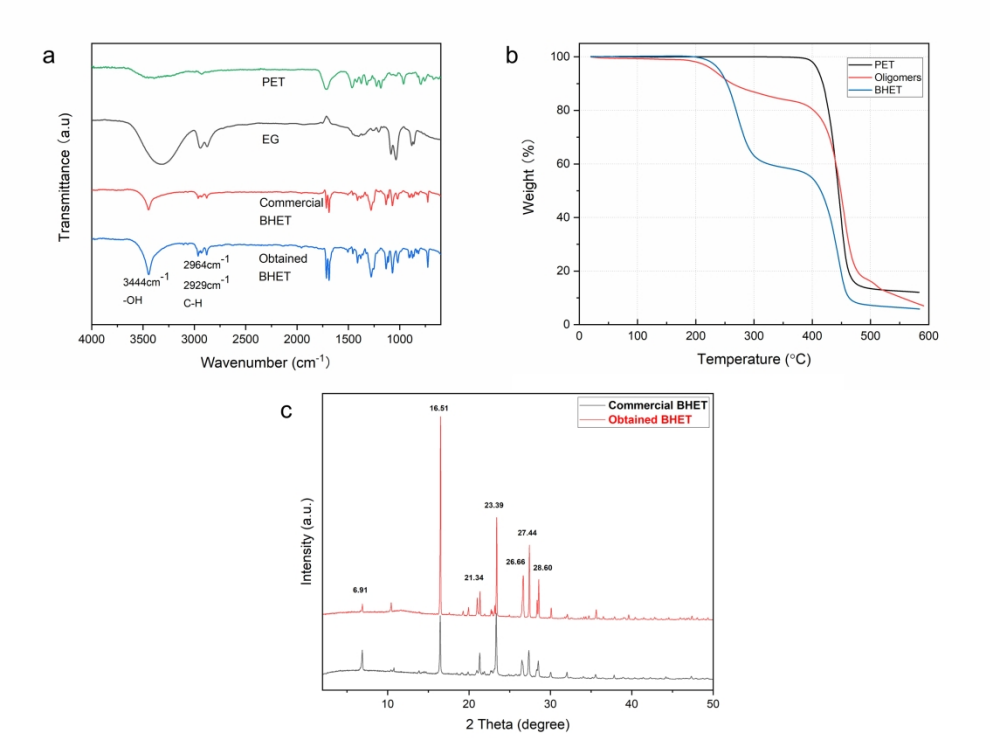

(a) FTIR spectra of PET, EG, commercial BHET, and BHET product obtained from the reaction. (b) TGA curves of PET, oligomers, and BHET produced from the reaction. (c) XRD spectra of commercial BHET and BHET product obtained from the reaction.

266x199mm (300 x 300 DPI)

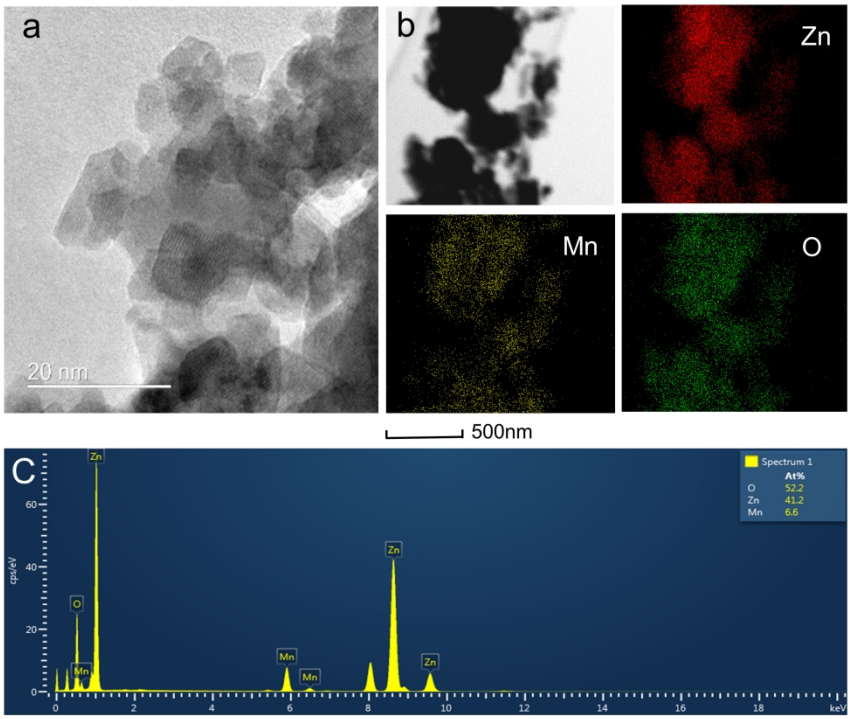

(a) TEM images of 10wt% Mn/ZnO. (b) EDX mapping images, (c) EDX sum spectrum of the surface of 10wt% Mn/ZnO.

242x190mm (300 x 300 DPI)

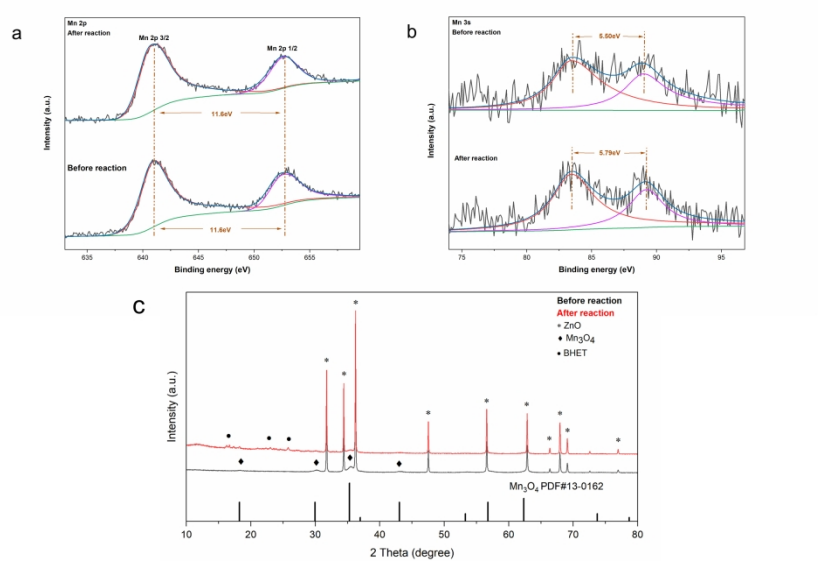

XPS and XRD spectra of Mn/ZnO before and after the reaction. (a) deconvolution of Mn 2p before and after reaction, (b) deconvolution of Mn 3s before and after reaction, (c) XRD spectra of 10wt% Mn/ZnO before and after reaction.

338x190mm (300 x 300 DPI)

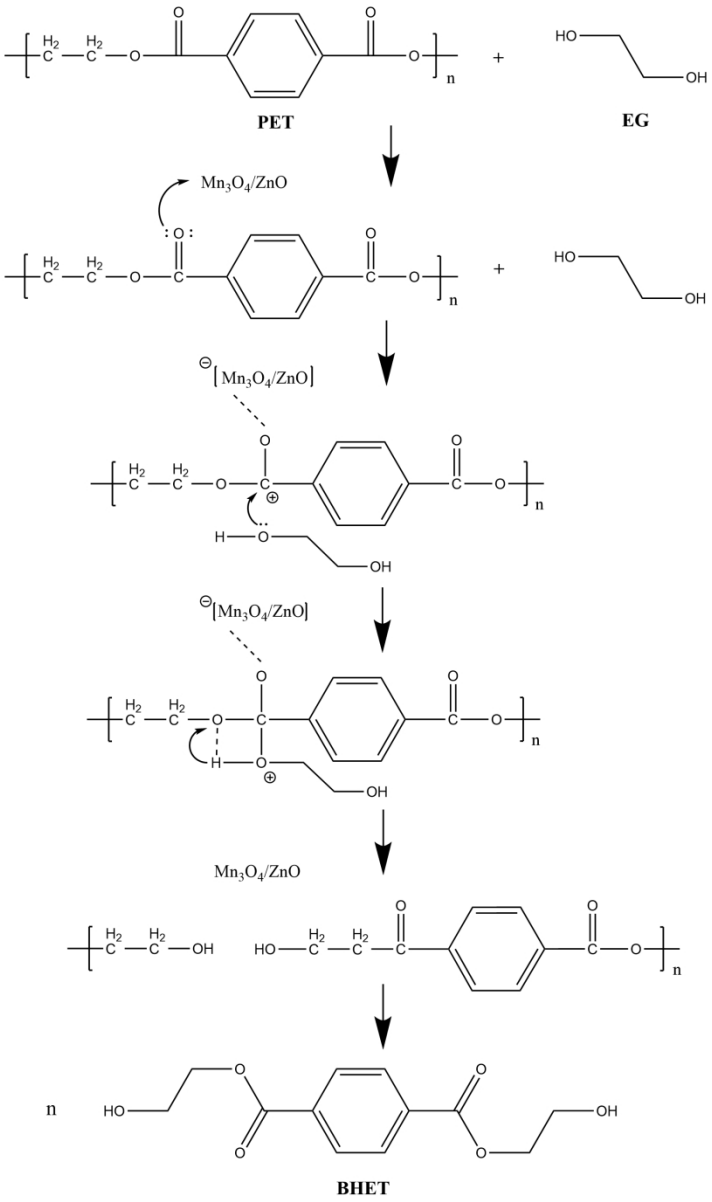

The proposed mechanism of the glycolysis of PET catalysed by 10 wt% Mn/ZnO.

153x258mm (300 x 300 DPI)

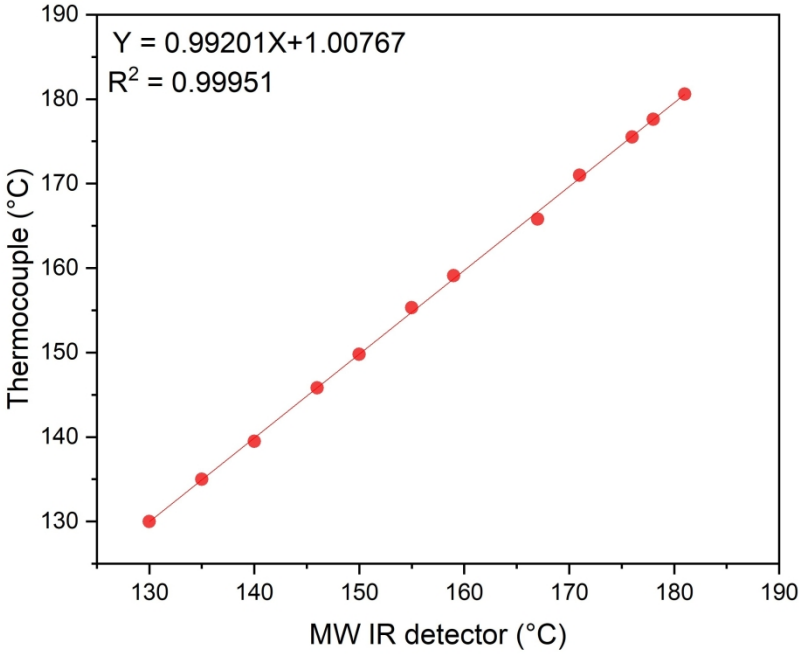

Calibration of MW IR temperature detector

272x208mm (300 x 300 DPI)

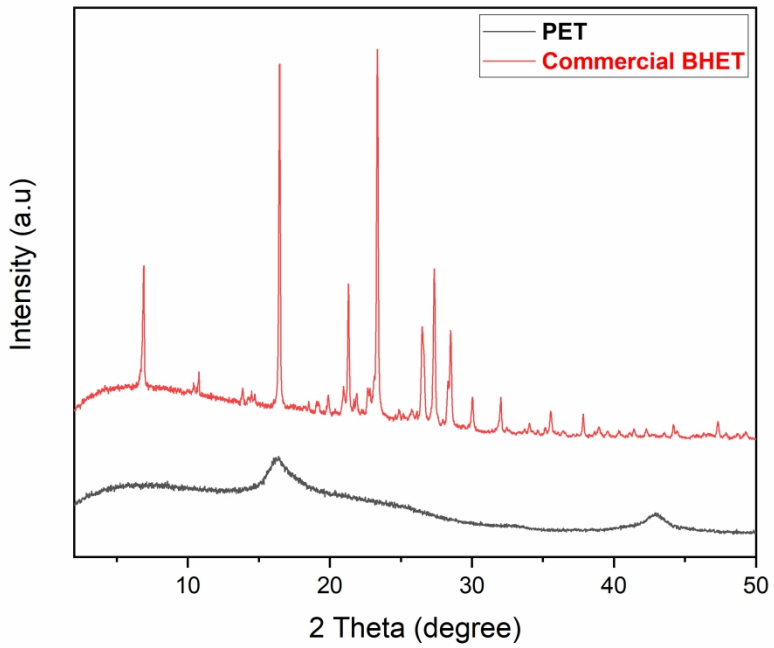

XRD spectra of PET and commercial BHET.

272x208mm (300 x 300 DPI)

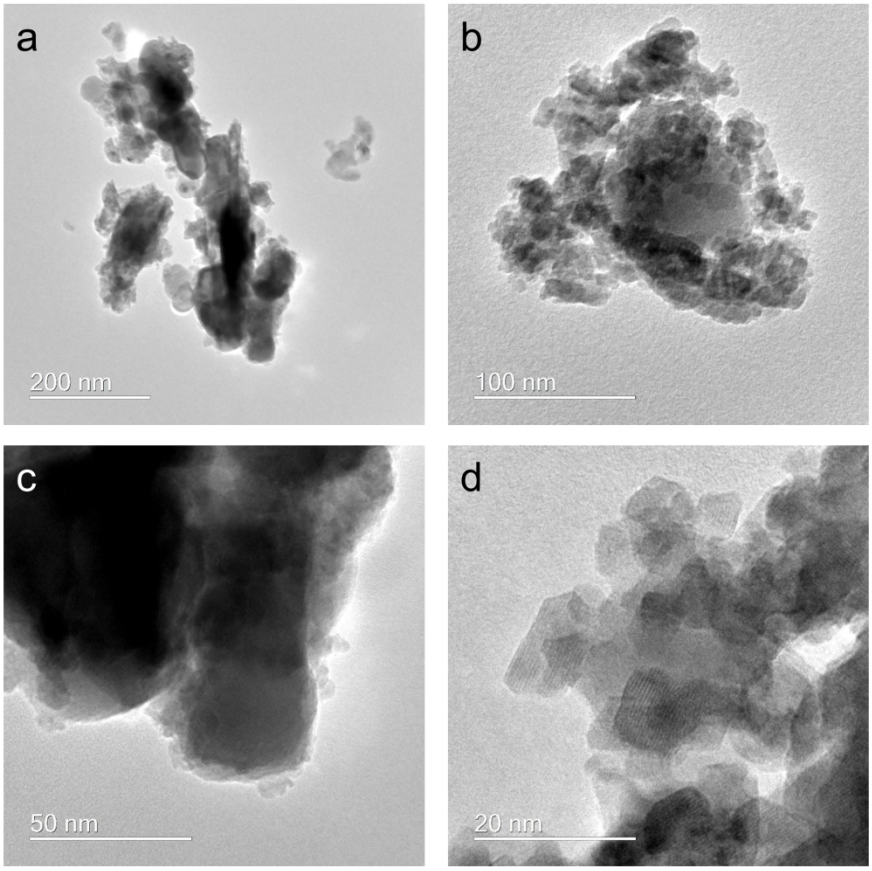

TEM images of 10wt% Mn/ZnO with different scales. (a) 200 nm. (b) 100nm. (c) 50nm. (d) 20nm.

207x189mm (300 x 300 DPI)